Drug Design, Development and Therapy

Dovepress
Taylor & Francis Group

Open Access Full Text Article

ORIGINAL RESEARCH

Preparation of 18β-Glycyrrhetinic Acid Liposome and Its Therapeutic Effect on Pulmonary Arterial Hypertension

Yanmin Pei[1,*], Meidong Si[1,*], Xuemei Ma[1], Siyun Liu[1], Fang Zhao[2], Ru Zhou[1,3,4]

[1]School of Pharmacy, Ningxia Medical University, Yinchuan, 750004, People's Republic of China; [2]Pediatric Intensive Care Unit, General Hospital of Ningxia Medical University, Yinchuan, Ningxia, 750004, People's Republic of China; [3]NHC Key Laboratory of Metabolic Cardiovascular Diseases Research, Ningxia Medical University, Yinchuan, 750004, People's Republic of China; [4]Ningxia Characteristic Traditional Chinese Medicine Modernization Engineering Technology Research Center, Ningxia Medical University, Yinchuan, 750004, People's Republic of China

*These authors contributed equally to this work

Correspondence: Fang Zhao, Pediatric Intensive Care Unit, General Hospital of Ningxia Medical University, Yinchuan, Ningxia, 750004, People's Republic of China, Tel/Fax +86 951 409 1488, Email ysj119zf@163.com; Ru Zhou, School of Pharmacy, Ningxia Medical University, Yinchuan, 750004, People's Republic of China, Tel/Fax +86 951 698 0192, Email zhou-ru926@163.com

Purpose: 18β-Glycyrrhetinic acid liposomes (18β-GA-Lips) were developed to enhance lung-specific drug delivery and optimize the therapeutic management of pulmonary arterial hypertension (PAH).

Methods: 18β-GA-Lips of varying particle sizes were formulated using the film-dispersion method and the thin-film dispersion-probe ultrasonic technique. Their characteristics, pharmacokinetics, and tissue distribution were thoroughly investigated, followed by an inhalation subacute toxicological analysis. Anti-PAH effects were assessed through hemodynamic measurements, right ventricular hypertrophy evaluation, echocardiography, histomorphometric, and morphological analyses.

Results: The 18β-GA-Lips, with varying particle sizes, exhibited a uniform spherical morphology, achieved entrapment efficiencies exceeding 80%, and had average particle sizes ranging from 150 to 1183 nanometers. These were categorized into four distinct size groups. The drug release profile demonstrated favorable sustained-release characteristics in vitro, and the formulation remained stable for up to 15 days when stored at 4°C. Pharmacokinetic analyses revealed that, compared with the 18β-GA-solution group, the $AUC_{(0\rightarrow48)}$, $MRT_{(0\rightarrow48)}$, $t_{1/2}$, t_{max}, and clearance rate of 18β-GA-Lips in each group were 4.42, 3.27, 4.28, 5.07, 2.10, 3.41, 1.73, 1.46, 1.53, 1.32, 1.79, 1.67, 0.61, 2.11, 0.71, 1.71, 1.15, 0.62, 0.96, and 0.90 times higher, respectively. Tissue distribution studies revealed that B-18β-GA-Lips exhibited the highest lung-targeting efficiency, with a Te value of 54.13%. No apparent signs of toxicity were observed. In vivo data demonstrate that rats treated with 18β-GA in different formulations (solution and liposomal) and with NO exhibited significantly lower mPAP and RVSP compared to the SuHx group, with no statistically significant differences observed among the treatment groups. Notably, 18β-GA-Lips exhibited a more pronounced reduction in RVHI compared to oral solutions and significantly attenuated pulmonary vascular remodeling. Furthermore, pharmacodynamic evaluations indicated that 18β-GA-Lips exhibited superior inhibitory effects on PAH in rats compared to both atomized and intragastric 18β-GA solutions.

Conclusion: These findings confirm that 18β-GA-Lips exhibit outstanding lung-targeting capabilities and lack inhalation toxicity, thereby significantly enhancing the therapeutic efficacy of treatments for PAH.

Keywords: 18β-glycyrrhetinic acid, liposomes, pharmacokinetics, lung targeting, pulmonary arterial hypertension

Introduction

Pulmonary Arterial Hypertension (PAH) remains a progressive and concerning pulmonary vascular disease, characterized by high mortality rates and long-term poor prognosis, often referred to as a "cardiovascular cancer".[1–4] The therapeutic outcomes of PAH have significantly improved with the advent of new targeted therapies, especially when compared to the 1980s. Despite the availability of these new therapies, none are capable of reversing pulmonary vascular remodeling, and PAH remains incurable.[5–7] The concept of pulmonary inhalation has been proposed for clinical application. Several

Received: 17 June 2025
Accepted: 28 October 2025
Published: 13 December 2025

drugs have currently been approved for inhalation therapy in the treatment of PAH, including iloprost, treprostinil, seralutinib, and fasudil solutions. These drugs target the lungs directly via inhalation, thereby reducing systemic side effects and enhancing local drug concentrations within the pulmonary tissue. However, these therapies have certain limitations, including a short duration of action (1–2 hours), the need for frequent administration (6–9 times per day), and the occurrence of side effects, which may lead to patient intolerance and persistently suboptimal therapeutic outcomes.[8,9]

Inhalation therapy is highly favored as a treatment modality because of its precise targeting, rapid onset of action, and ability to achieve superior therapeutic effects at lower drug doses. In recent years, with advancements in inhalation therapy research, a new generation of inhaled therapeutic agents has emerged. For example, inhaled treprostinil has been shown to improve patient survival rates and, due to its high stability, significantly enhance long-term prognosis and quality of life.[8] Moreover, liposomal drug delivery systems—particularly liposomal treprostinil (L606), currently undergoing clinical trials—represent a promising strategy to enhance pulmonary targeting and prolong the duration of action. These liposomes facilitate sustained drug release within the lungs while protecting the active compound from rapid metabolism. The potential to reduce dosing frequency and enhance therapeutic efficacy may provide patients with more convenient and effective treatment options. Therefore, to improve the treatment of PAH, it is crucial to reform traditional dosage forms and develop lung-targeted formulations for more precise treatment of PAH.

Liposomes are a widely studied drug delivery system for aerosolized inhalation in the lungs.[10] Liposomal aerosolized inhalation combines its inherent advantages and localized drug delivery characteristics, allowing for slow release in the lungs, maximizing transfer and deposition.[11,12] Particle size is a key factor in determining whether liposomal aerosolized inhalation reaches the lungs. Theoretically, only particles with an aerodynamic diameter between 500 nm and 5000 nm can be deposited in the lungs. Particles larger than 5000 nm will remain in the oropharynx, while particles smaller than 500 nm will mostly be exhaled with the breath.[13,14] Our goal is to control the liposome particle size to ensure the drug reaches the alveolar region, provides sustained retention time and cellular fusion, minimizes distribution to other tissues, and reduces adverse reactions.

Glycyrrhiza glabra L. is a characteristic leguminous medicinal plant native to Ningxia. Glycyrrhetinic acid (GA) is a triterpene compound formed by the hydrolysis of two glucuronic acid molecules from glycyrrhizic acid, with 18β-GA accounting for 97% of GA. It is easier to synthesize and extract than other bioactive components of *Glycyrrhiza*.[15] 18β-GA has been shown to possess antioxidant and other pharmacological activities in various animal models. Preliminary results from our research group indicate that 18β-GA inhibits the RhoA/ROCK signaling pathway and oxidative stress to treat MCT-induced PAH in rats.[16,17] 18β-GA is classified as a low solubility, high permeability Class II drug in the Biopharmaceutical Classification System and exhibits aldosterone-like effects when administered at high doses over extended periods.[18,19] To maintain the therapeutic efficacy of glycyrrhizic acid and reduce side effects, 18β-glycyrrhizic acid topical gel,[20] 18β-glycyrrhizic acid encapsulation,[21] and 18β-glycyrrhizic acid nanocrystals[22] with glycyrrhizic acid as the main drug delivery system have been developed in recent years, but there are still potential problems such as immunogenicity and low potency. Therefore, in order to improve the treatment of PAH, it is crucial to modify the traditional dosage forms and prepare lung-targeted formulations to achieve precise treatment of PAH. Liposomes are nano-formulations with a bilayer structure, which have the advantage of high biocompatibility, improved drug solubility, and increased localisation of treatment to diseased tissues as a carrier for drug delivery, which in turn may improve efficacy. In addition, their use is widely recognised in all types of diseases and in all forms of drug delivery. It is anticipated that liposomes will be used as a more effective formulation to mitigate the side effects of 18β-GA.

In this study, we aimed to determine whether 18β-GA-liposomes (18β-GA-Lips) exhibit lung-targeting efficiency and an anti-PAH effect. First, 18β-GA, an effective anti-PAH agent from traditional Chinese medicine, was used as the model drug, and 18β-GA-Lips with varying particle sizes were prepared. The physicochemical properties of 18β-GA-Lips, including in vitro release efficiency, were characterized. Additionally, we investigated the pharmacokinetics and lung-targeting profile of 18β-GA-Lips using Ultra Performance Liquid Chromatography Tandem Mass Spectrometry (UPLC/MS). Finally, a comparison was made with oral intragastric administration of 18β-GA solution to verify whether aerosolized 18β-GA-Lips are more effective in treating PAH. We anticipate that 18β-GA-Lips will improve lung-targeting efficiency and enhance the clinical treatment of PAH.

Materials and Methods

Animals

Male ICR mice (20 ± 2 g, 6 weeks old) and male Sprague-Dawley rats (SD rats, 220–250 g, 6 weeks old) were obtained from the Animal Experimental Center of Ningxia Medical University (SYXK Ningxia 2015–0001). The animal use protocol outlined below was reviewed and approved by the Laboratory Animal Ethical and Welfare Committee of the Laboratory Animal Center, Ningxia Medical University (IACUC-NYLAC-2020-015). All rodents were housed in an animal room maintained at 20 ± 2°C with a humidity of 50–60%. The light/dark cycle was set to 12 hours, and the animals had free access to food and water. The animal room is situated in the Key Laboratory of Ningxia Ethnic Medicine Modernization at Ningxia Medical University. All procedures related to feeding, modeling, administration, anesthesia, and other operations involving rats and mice in this experiment were conducted in the Key Laboratory of Ningxia Ethnic Medicine Modernization at Ningxia Medical University, which is an SPF-level environment. The study was conducted in accordance with the policies outlined in Basic & Clinical Pharmacology & Toxicology for experimental and clinical studies.[23]

Reagents

18β-GA, with a purity greater than 98.0% as confirmed by HPLC analysis, was purchased from Yuan Ye Biotechnology Co., Ltd. (Shanghai, China, Cat. No. S31512). The glycyrrhetinic acid standard was purchased from the China Institute for Food and Drug Control (Beijing, China, Cat. No. L6PM-GVAA). Hydrogenated soybean phospholipid (HSPC, Cat. No. C00257), cholesterol (CHOL, batch number: B80859), and distearoyl phosphatidylethanolamine polyethylene glycol 2000 (DSPE-MPEG2000, Cat. No. B90396) were purchased from AVT Pharmaceutical Technology Co., Ltd. (Shanghai, China). N-2-hydroxyethyl piperazine-N′-2-ethanesulfonic acid (HEPES) was purchased from Shanghai Yien Chemical Technology Co., Ltd. (Shanghai, China, Article No. RO11833). Sodium dodecyl sulfate (SDS) was purchased from Beijing Solebao Technology Co., Ltd. (Beijing, China, Cat. No. 20181010). Lansoprazole standard was purchased from the China Institute of Pharmaceutical and Biological Products Identification (Beijing, China, Cat. No. 100709–200902). SU5416 was provided by Medkoo Biosciences (North Carolina, USA).

Experimental Design

Formulation of Liposome-18β-GA

Liposomes were prepared using the film-dispersion method[24] and the thin-film dispersion-probe ultrasonic method[25] (All primary experimental instruments and equipment, including their respective models and manufacturers, are detailed in Table S1).

Film-Dispersion Method

Accurately weighed the prescribed amounts of HSPC, CHOL, and DEPE-MPEG2000 excipients and placed them in a 50 mL round-bottom flask. Added an appropriate amount of chloroform and methanol to dissolve the excipients. Next, accurately weighed the prescribed amount of 18β-GA and placed it in another 50 mL round-bottom flask, adding the same volume of chloroform and methanol. After magnetic stirring for 2 hours (800 rpm) at room temperature, combined the two solutions and continued magnetic stirring for an additional 2 hours (800 rpm) at room temperature. The chloroform-methanol mixture was then removed using a rotary evaporator (water bath temperature: 40°C, rotation speed: 25 rpm) to form a uniform, transparent film on the walls of the flask. The film was subsequently stored in a refrigerator at 4°C for 72 hours. An appropriate volume of pre-prepared HEPES buffer solution (pH 7.4) was added to the film, followed by magnetic stirring at 37°C for 4 hours to hydrate the lipid film. Finally, the suspension was filtered through a 0.8 μm organic microporous filter membrane to obtain the 18β-GA liposome suspension.

Thin-Film Dispersion-Ultrasonic Probe Method

Accurately weighed the prescribed amounts of HSPC, CHOL, and DEPE-MPEG2000 excipients into a 50 mL round-bottom flask, added an appropriate amount of trichloromethane and methanol to dissolve. Then, accurately weighed the prescribed amount of 18β-GA into a separate 50 mL round-bottom flask, added equal volumes of trichloromethane and

methanol, and stirred magnetically for 2 hours (800 rpm) at room temperature. The mixture was then evaporated using a rotary evaporator (water bath temperature of 40°C) to remove the trichloromethane and methanol, forming a uniform, transparent film on the flask wall. Equal volumes of trichloromethane and methanol were added, and the mixture was stirred magnetically for 2 hours (800 rpm) at room temperature. The solvent was removed using a rotary evaporator (40°C, 25 rpm/min), forming a uniform, transparent film on the flask wall. The film was then placed in a refrigerator at 4°C for 72 hours. An appropriate volume of pre-equilibrated HEPES buffer (pH 7.4) was added to the membrane suspension, and the sample was sonicated with an ultrasonic cell disruptor in an ice bath for 10 minutes at a power setting of 200 W and an amplitude of 40%. The sample was then filtered through a 0.8 μm organic microporous filter membrane. The 18β-GA liposome suspension was then filtered through a 0.8 μm organic microporous filter membrane and stored at 4°C.

Formulation optimization was carried out by varying the ratios between different compositions and adjusting the sonication duration (Tables S2–S4). This was done to determine several formulations of 18β-GA-Lips with different particle sizes (A-18β-GA-Lips, B-18β-GA-Lips, C-18β-GA-Lips, D-18β-GA-Lips).

Liposome Characterization

Transmission Electron Microscopy

The morphology of 18β-GA-Lips was observed using Transmission Electron Microscopy (H-7650, HITACHI, Tokyo, Japan). The liposomes were then diluted, placed on copper grids, and stained with 2% phosphotungstic acid for further analysis.

Z-Average Size, Zeta Potential, and Polydispersity Index

Z-The average size, zeta potential, and Polydispersity Index (PDI) of 18-GA-Lips were measured using a Zetasizer instrument (ZS90, Malvern Instrument Co., Ltd).

Encapsulation Efficiency and Drug Loading

For each group of 18β-GA-Lips (n=3), 9.9 mL of DMSO was added for demulsification, followed by vortexing for 5 minutes and ultrasonic treatment for 30 minutes. This process was repeated three times. The mixture was then diluted with 50% methanol–water, and the sample was injected into the chromatography system to measure the encapsulated concentration of 18β-GA (C_1), with measurements performed in triplicate for each sample.[26]

$$\text{Encapsulationefficiency} = \frac{(C_1 \times \text{DilutionFactor})}{\text{Dosage}} \times 100\%$$

$$\text{Drugloading} = \frac{(C_1 \times \text{DilutionFactor})}{(\text{Dosage} + \text{ExcipientsDosage})} \times 100\%$$

In vitro Drug Release

In vitro drug release from 18-GA-Lips was analyzed via dialysis against PBS (pH 7.4, 0.5% SDS) at 37°C under sink conditions. Briefly, 1 mL of 18-GA-Lips and free 18-GA (containing 1 mg of the drug) were placed in separate dialysis bags with a molecular weight cutoff of 14 kDa, sealed, and immersed in 250 mL phosphate-buffered saline (pH 7.4, 0.5% SDS), separately. The medium was stirred at 37°C. At predetermined time intervals (0.25, 0.5, 1, 2, 4, 6, 8, 12, 24, and 48 hours), 3 mL of medium was withdrawn and replaced with an equal volume of fresh medium. Samples were filtered through a 0.45 μm syringe filter, injected into the HPLC system, and analyzed using the aforementioned HPLC method. All measurements were performed in triplicate. The same method was applied to 18β-GA API.

Stability Study

Liposome stability under in vitro storage conditions is a critical criterion for both in vitro and in vivo biomedical applications. The stability of the liposomes was evaluated[27] at 7, 15, 30, and 60 days after Formulation and storage at 4°C.

In vivo Pharmacokinetic Study

An in vivo pharmacokinetic study was conducted as previously described. Briefly, Thirty SD rats (220–250 g, 6 weeks old) were randomly assigned to five groups (n = 6): 18β-GA solutions, 18-GA-Lips with a particle size of 1200 nm (A-18β-GA-Lips), 18β-GA-Lips with a particle size of 800 nm (B-18β-GA-Lips), 18-GA-Lips with a particle size of 400 nm (C-18β-GA-Lips), and 18-GA-Lips with a particle size of 200 nm (D-18β-GA-Lips). Each group was aerosolized with a dose of 25 mg/kg. Approximately 0.5 mL of blood was collected from the rats' inner canthus before and after administration at 0.083, 0.25, 0.5, 1, 2, 4, 6, 8, 10, 12, 24, and 48 h, The blood samples were placed in heparinized centrifuge tubes, centrifuged at 4000 rpm for 10 minutes at 4°C. The concentration of 18β-GA in plasma was measured by UPLC-MS/MS (Shimadzu 30A / API 4000 quadrupole tandem mass spectrometer, Shimadzu, Japan / Applied Biosystems, USA). The relevant instrument parameters are shown in Tables S5 and S6, and the analysis was performed according to the mass spectrometry and chromatographic conditions. The experimental data obtained were used to construct the blood drug concentration–time curve, and the data were processed using the non-compartmental model in DAS 2.0 pharmacokinetic software.

In vivo Biodistribution Study

Two hundred and forty male ICR mice (20 ± 2 g, 6 weeks old) were randomly divided into five groups (n=48 per group) and administered 18β-GA solutions, 18β-GA-Lips with a particle size of 1200 nm (A-18β-GA-Lips), 18β-GA-Lips with a particle size of 800 nm (B-18β-GA-Lips), 18β-GA-Lips with a particle size of 400 nm (C-18β-GA-Lips), or 18β-GA-Lips with a particle size of 200 nm (D-18β-GA-Lips), aerosolized at a dose of 35 mg/kg of 18β-GA, respectively. After the specified time points (0.5, 1, 2, 4, 6, 12, 24, and 48 hours), the mice were sacrificed by dislocation of the cervical spine (n = 6 per time point). The tissues (heart, liver, spleen, lung, kidney, and brain) were then collected, weighed (0.2–0.3 g), and 800 μL of normal saline (NS) was added. The tissues were then placed in a grinding tube for homogenization. Samples were immediately frozen at −20°C and analyzed within 3 days.

The concentration of 18β-GA in the organization was measured by UPLC-MS/MS (Shimadzu 30A / API 4000 quadrupole tandem mass spectrometer, Shimadzu, Japan / Applied Biosystems, USA), with the relevant instrument parameters as described above. The concentration–time distribution characteristics of each tissue were then plotted. The non-compartmental model in DAS 2.0 pharmacokinetic software was used to process the data, calculate the main pharmacokinetic parameters, and determine the target parameters based on the pharmacokinetic data: target efficiency (Te), relative target efficiency (RTe), relative uptake rate (Re), and peak concentration ratio (Ce).

$$\mathrm{Te} = \frac{\mathrm{AUC}_{\mathrm{Targettissue}}}{\mathrm{AUC}_{\mathrm{Total}}} \tag{1}$$

$$\mathrm{R}_{\mathrm{Te}} = \frac{\mathrm{Te}_{\mathrm{Experiencegroup}}}{\mathrm{Te}_{\mathrm{Controlgroup}}} \tag{2}$$

$$\mathrm{Re} = \frac{\mathrm{AUC}_{\mathrm{Experiencegroup}}}{\mathrm{AUC}_{\mathrm{Controlgroup}}} \tag{3}$$

$$\mathrm{Ce} = \frac{\mathrm{Cmax}_{\mathrm{Experiencegroup}}}{\mathrm{Cmax}_{\mathrm{Controlgroup}}} \tag{4}$$

The Effects of Subacute Inhalation Toxicity of 18β-GA Liposomes

Fifty SD rats (220–250 g, 6 weeks old) were randomly divided into five groups (n=10). The control group consisted of two subgroups, which were atomized with physiological saline for 14 days and 21 days, respectively. The low-dose group (F group) was atomized with 18β-GA-Lips at a dose of 25 mg/kg for 14 days. The high-dose groups (E group and G group) were treated as follows: The E group was atomized with 18β-GA-Lips at 100 mg/kg for 14 days, and the G group was atomized for 21 days. Atomized administration was performed once a day.

Observation of Clinical Symptoms in the Rats

During the experiment, the general behavior of the rats was observed daily, including checking for signs of panic, convulsions, ataxic gait, abnormal diet, defecation, sensitivity to stimulation, stool properties and color, as well as examining the skin, mucous membranes, respiration, heartbeat, fur, eyes, nose, and limbs for abnormalities. Additionally, observations were made to determine whether the tested animals exhibited signs of poisoning, and whether there were any records of deceased animals.

Record Changes in Weight and Food Intake of Rats

The rats were weighed at the same time each week, and their food intake and surplus were recorded every two days to calculate the total food intake.

Functional Observation Battery (FOB) Test

During the administration period, functional observation combination tests were conducted once a week in each dose group of rats to observe changes in 23 indicators: awakening, grooming, panic, posture, twitching, tail posture, urination, defecation, upright posture, cyanosis, salivation, inability to open eyes, proptosis, tearing, blood in tears, pupillary reaction, autonomous movement, ataxic gait, finger approach, head touch, righting reflex, sensitivity to tail pinching, and panic reaction.

Analysis of Blood Indicators in Rats

After the final atomization, Fifty SD rats (220–250 g, 6 weeks old) were fasted for 12 hours and then treated with water. 2% pentobarbital sodium was administered intraperitoneally for anesthesia (2 g of pentobarbital sodium was dissolved in 100 mL of normal saline). Approximately 10 mL of blood was collected from the abdominal aortic vein of each rat. Haematological analysis of the blood was performed. The blood was divided into two portions: one was placed in anticoagulant tubes containing EDTA-Na2, and the other in non-anticoagulant tubes. The blood in the anticoagulant tubes was used for routine blood testing. The non-anticoagulant tubes were stored at 4°C overnight, and the upper serum was then collected for the determination of blood biochemical markers. Blood samples were collected into 1.5 mL centrifuge tubes and stored at 4°C for 30–60 minutes. The samples were then centrifuged at 3000 rpm at 4°C for 15 minutes. Finally, the supernatant (serum) was collected into a centrifuge tube for testing of the following parameters: white blood cell count (WBC), red blood cell count (RBC), hemoglobin (HGB), hematocrit (HCT), platelet count (PLT), mean platelet volume (MPV), plateletcrit (PCT), mean corpuscular volume (MCV), mean corpuscular hemoglobin (MCH), mean corpuscular hemoglobin concentration (MCHC), red blood cell distribution width (RDW), platelet distribution width (PDW), and large platelet ratio.

Analysis of Biochemical Indicators in Rats

Blood biochemical indicators such as Aspartate transaminase (AST), alanine aminotransferase (ALT), total bilirubin (T-BIL), direct bilirubin (D-BIL), indirect bilirubin (IBIL), total protein (TP), Alkaline phosphatase (ALP), globulin (GLB), white/ball ratio (A/G), glutamyltransferase (GGT), urea (BUN), creatinine (CRE), Glucose (GLU), Triglycerides (TG), Total cholesterol (TCHO), High-density lipoprotein cholesterol (HDL-C), Low-density lipoprotein cholesterol (LDL-C), Creatine kinase (CK), cholinesterase (CHE), Inorganic phosphorus (IP), Lactate dehydrogenase (LDH), total Bile acid (TBA), Uric acid (UA).

Analyze Rat Urine Indicators

After the final atomization, the experimental animals were administered water following a 12-hour fasting period. Each rat was individually placed in a metabolic cage to collect urine. The following parameters were analyzed and detected using a urine analyzer: specific gravity, vitamin C (G/L), WBC, nitrite (NIT), pH, occult blood, protein (PRO), glucose (GLU), ketone bodies (KET), urobilinogen (URO), and bilirubin (BIL).

Perform B-Mode Ultrasound Examination in Rats

After the final administration, ultrasonic cardiogram images and data of the rats were recorded using a GE VIVID7 (General Electric Company, USA), including HR, systolic blood flow velocity (VS), diastolic blood flow velocity (VD), stroke volume (SV), left ventricular ejection fraction (EF%), left ventricular shortening fraction (FS%), stroke output (CO), left ventricular mass (LV Mass), and others. The wall thickness of the right ventricle and the internal diameter of the right ventricle during systole and diastole were measured using M-mode echocardiography. The maximum pulmonary blood flow velocity (PVmax), pulmonary artery acceleration time (PAAT), and pulmonary artery deceleration rate (PAD) were assessed using Doppler vascular ultrasound.

Histopathological Examination in Rats

During the experiment, if any abnormalities or deaths occur, the rats will be euthanized and sampled for gross anatomical examination. Pathological examination: After the final aerosol administration, the experimental animals were fasted for 12 hours and then treated with water. Following weighing, 2% pentobarbital sodium was administered intraperitoneally for anesthesia (2 g of pentobarbital sodium was dissolved in 100 mL of normal saline). First, observe for visible lesions in each organ of the rats. The heart, liver, spleen, lungs, kidneys, brain, rectum, testes, epididymides, muscles, skin, bones, and spinal cord were fixed in paraformaldehyde, and H&E staining was performed for pathological examination.

Therapeutic Effects of 18β-GA Solutions and 18β-GA-Lips on PAH

Forty-two male SD rats (220–250 g, 6 weeks old) were randomly divided into seven groups: control group (n = 6), model group (SuHx, n = 6), 18β-GA solutions group (SuHx + atomized 18β-GA solution, 6.25 mg/kg/day, n = 6), 18β-GA-Lips group (SuHx + atomized 18β-GA-Lips, 6.25 mg/kg/day, n = 6 and 50 mg/kg/day, n = 6), 18β-GA solutions intragastric group (SuHx + intragastric 18β-GA solution, 100 mg/kg/day, n = 6), and NO group (SuHx + NO, n = 6). Modeling began on the first day following Su5416 injection (20 mg/kg, subcutaneously). From day one, nitrogen flow was adjusted to maintain an O_2 concentration of 10% in the low-oxygen compartment for 3 weeks, and the rats were placed in the compartment. Sodium lime and anhydrous calcium chloride were placed in the compartment to absorb water and carbon dioxide generated within. After modeling, rats in each experimental group received atomization of 18β-GA solutions (6.25 mg/kg/day), atomization of 18β-GA-Lips (6.25 mg/kg/day and 50 mg/kg/day), intragastric administration of 18β-GA solutions (100 mg/kg/day), and atomization of NO (30 min/day) for 3 weeks. The same volume of NS was administered to the control and SuHx groups.

Echocardiographic Analysis

Prior to the examination, all rats were anesthetized with 2% sodium pentobarbital via intraperitoneal injection (2 g of pentobarbital sodium dissolved in 100 mL of normal saline). After chest shaving, echocardiographic parameters were measured using a GE Vivid7 color Doppler ultrasound diagnostic system (General Electric, CO, USA). Doppler signals of the pulmonary artery valve blood flow pulse wave were obtained from the parasternal short-axis left ventricular section. PAAT and PVmax were measured, along with the end-systolic diameter of the right ventricle (RVESD). All echocardiographic measurements and parameters were recorded and stored by the same person under anesthesia, with a heart rate maintained at 350–400 bpm.

Hemodynamic Measurements

The rats were weighed and recorded 4 weeks after the modeling procedure. A 20% urethane solution was prepared for anesthesia (20 g of urethane dissolved in 100 mL of normal saline). Based on the rats' weight, 20% urethane (1 mL/100 g) was administered intraperitoneally for right cardiac catheterization anesthesia. Once the anesthesia was stable, the right external jugular vein was isolated, and an arc catheter was inserted into the vein, advanced toward the heart. The catheter was gently rotated to adjust its direction, and its location was confirmed by the pressure waveform. Once the catheter slowly entered the right ventricle, the pressure waveform was recorded. The catheter was then advanced into the pulmonary artery, and the pressure waveform was recorded again.

Evaluation of Right Ventricular Hypertrophy

After the hemodynamic measurements, the rats were euthanized. The rats were then exposed to the thoracic cavity, and the heart and lungs were carefully removed. They were washed with normal saline, and excess water was blotted with filter paper. The right ventricle (RV) and left ventricle + inter-ventricular septum (LV + S) were separated and weighed. The right ventricular hypertrophy index (RVHI) was calculated as follows: RVHI = right ventricle weight / (left ventricle + inter-ventricular septum weight) (RV / LV + S).

Histomorphometric Analysis

H&E Staining. Tissue from the lower lobe of the left lung was excised and fixed in 4% paraformaldehyde for 48 hours. Paraffin sections were prepared, followed by dewaxing, rehydration, and hematoxylin and eosin (H&E) staining. Histological images of pulmonary microvessels measuring less than 200 μm were captured and analyzed using a light microscope. The pulmonary artery remodeling index was calculated using the following formulas: (1) wall thickness ratio (WT%) = 100% × (external diameter − internal diameter)/external diameter, and (2) wall area ratio (WA%) = 100% × (cross-sectional wall area − lumen area)/cross-sectional wall area.

Morphological Assessment Using an Electron Microscope. A sample of left lung tissue was pre-fixed in Bouin's fixative at 4°C for 2 hours, then cut into 1 mm × 1 mm × 1 mm cubes, which were subsequently fixed again, dehydrated, embedded into slices, and stained with uranyl acetate and lead citrate. Histopathological changes in the lung tissue were observed under an electron microscope (Olympus, Tokyo, Japan, 12,000×), and representative images were captured.

Statistical Analysis

Results are presented as mean ± standard deviation (Mean ± S.D., n = 6). Data were analyzed using analysis of variance (ANOVA) and Student's *t*-test in SPSS 26.0 software. In all statistical tests, $P < 0.05$ was considered statistically significant.

Results

Single-Factor Experimental Analysis of 18β-GA-Lips Results

Based on the single-factor experiments examining different molar ratios of excipients, ultrasonic duration, and ultrasonic power, the Formulation process was optimized to yield four formulations with varying particle sizes (A-18β-GA–Lips, B-18β-GA–Lips, C-18β-GA–Lips, and D-18β-GA–Lips; Table 1). The optimization used particle size as the evaluation index (Tables S7–S9).

Characteristics of 18β-GA-Liposomes

Z-Average Size, Zeta Potential, Polydispersity Index, Encapsulation Efficiency, and Drug Loading Analysis

The average size, zeta potential, PDI, the encapsulation efficiencies (EE), and the drug loadings (DL) of 18-GA-Lips in each group are summarized in Table 2. The average sizes of 18-GA-Lips were 1183.00 ± 28.47 nm, 735.90 ± 61.40 nm, 383.33 ± 35.89 nm, and 150.17 ± 5.32 nm, respectively (Figure 1A–1D). These sizes were consistent with the enhanced permeability

Table 1 Optimal Prescription

Groups	HSPC:CHOL: DSPE-MPEG2000)	18β-GA	Size(nm)	Formulation Process
A-18β-GA–L	8.5:1:0.5	12	1193	The film dispersion method: The excipients and the drug are dissolved in chloroform and methanol. The dispersion medium is removed by rotary evaporation at 40 °C. HEPES buffer solution is added. The hydration is carried out at 37 °C for 4 hours. The mixture is then passed through a 0.8 μm organic membrane to obtain the final product.
B-18β-GA–L	7:2:1	12	663	
C-18β-GA–L	6:2:2	12	372	Film dispersion-probe ultrasonic method: The excipients and the drug are dissolved in chloroform and methanol. The dispersion medium is removed by rotary evaporation at 40 °C. HEPES buffer solution is added, and ultrasonic treatment is carried out at 200 W for 10 minutes. The mixture is then passed through a 0.8 μm organic membrane to obtain the final product.
D-18β-GA–L	7:2:1	12	158	

Table 2 Prescription Particle Size and Zeta Potential of Each Liposome Group (Mean ± S.D., n = 3)

Groups	Average Size (nm)	Zeta Potential (mV)	PDI	EE (%)	DL (%)
A-18β-GA–L	1183.00±28.47	−8.10±0.46	0.12±0.04	84.41±0.30	16.16±0.60
B-18β-GA–L	735.90±61.40	−9.25±0.32	0.13±0.01	88.42±0.94	13.20±1.40
C-18β-GA–L	383.33±35.89	−8.20±0.07	0.08±0.03	87.39±0.31	15.74±0.56
D-18β-GA–L	150.17±5.32	−16.57±0.87	0.08±0.05	85.76±1.74	12.80±2.60

and retention (EPR) effect, suggesting the potential for passive and active targeting to the lung area. The PDI values were below 0.2, indicating that the particle size distribution was relatively narrow. The zeta potentials, a key factor in evaluating the stability of liposome dispersion, were measured as −8.10 ± 0.46 mV, −9.25 ± 0.32 mV, −8.20 ± 0.07 mV, and −16.57 ± 0.87 mV for 18-GA-Lips (Figure 2A–D). 18-GA-Lips with an absolute zeta potential value greater than 20 mV exhibit relatively strong repulsive interactions and are considered stable. For the prepared 18-GA-Lips, EE were 84.41 ± 0.30%, 88.42 ± 0.94%, 87.39 ± 0.31%, and 85.76 ± 1.74%, while DL were 16.16 ± 0.60%, 13.20 ± 1.40%, 15.74 ± 0.56%, and 12.80 ± 2.60%. Based on these results, it was concluded that the size and zeta potential of 18-GA-Lips prepared using the film-dispersion method and the thin-film dispersion-probe ultrasonic method are satisfactory.

Observation Results of the Morphology of 18β-GA Lips

The morphological characteristics of A-18β-GA-Lips, B-18β-GA-Lips, C-18β-GA-Lips, and D-18β-GA-Lips were directly analyzed using Transmission Electron Microscopy (TEM). As shown in Figure 3A–D, the particles were spherical, with sizes ranging from 120 to 1200 nm, and exhibited no aggregation or fusion.

In vitro Release Analysis

The in vitro release profiles of free-18β-GA, A-18β-GA-Lips, B-18β-GA-Lips, C-18β-GA-Lips, and D-18β-GA-Lips are illustrated in Figure 4. The results indicated that within the first 12 hours, the in vitro release rate of free-18β-GA was significantly faster than that of all 18β-GA-Lips. The release rate reached 27.43% at 12 hours and 40.74% at 24 hours, after which it stabilized. However, the release profiles of 18β-GA-Lips across the other groups exhibited similar trends. The release rates of 18β-GA-Lips reached 55.02% to 68.37% at 24 hours, achieving complete release by 48 hours. The dissolution behavior of 18β-GA-Lips was significantly superior to that of the 18β-GA solution. These findings suggest that drug release is delayed after encapsulation within liposomes.

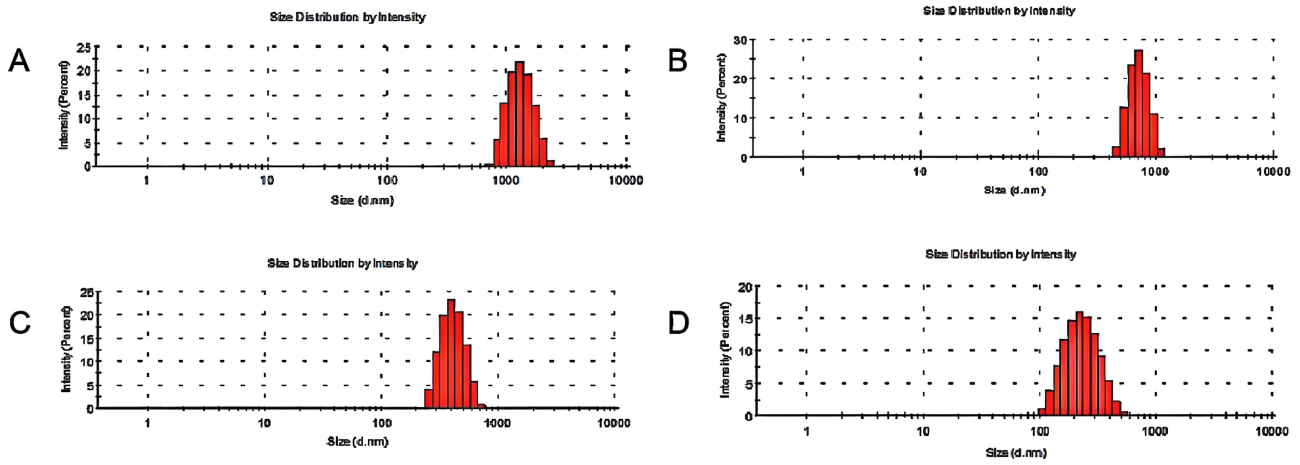

Figure 1 Particle Size Distribution of 18β-GA-Lips: ((**A**) A-18β-GA-Lips; (**B**) B-18β-GA-Lips; (**C**) C-18β-GA-Lips; (**D**) D-18β-GA-Lips).

https://doi.org/10.2147/DDDT.S547530

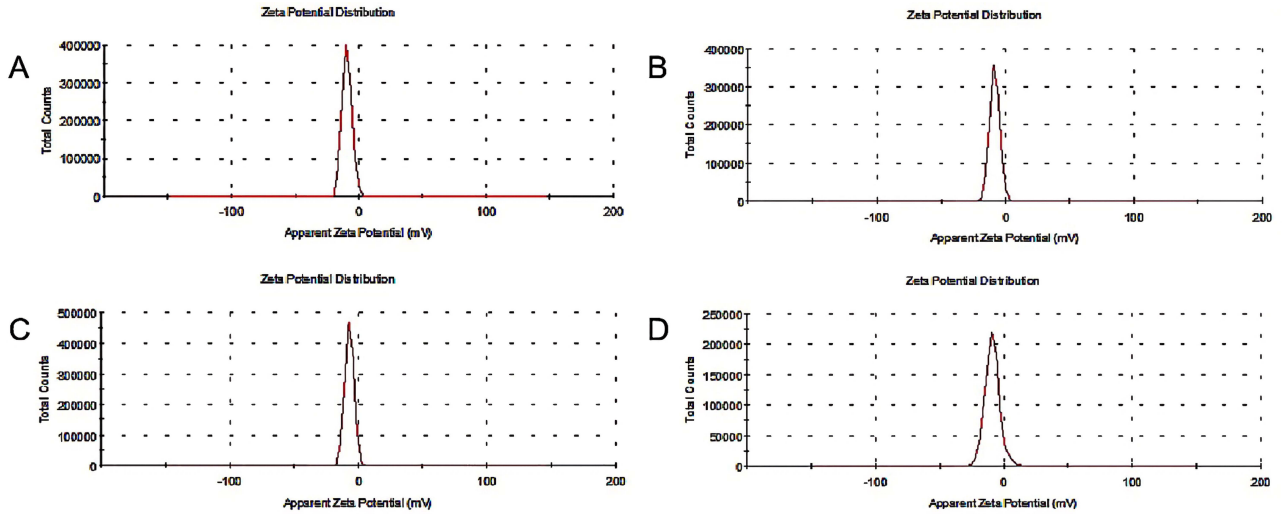

Figure 2 Potential Distribution of 18β-GA-Lips: ((**A**) A-18β-GA-Lips; (**B**) B-18β-GA-Lips; (**C**) C-18β-GA-Lips; (**D**) D-18β-GA-Lips).

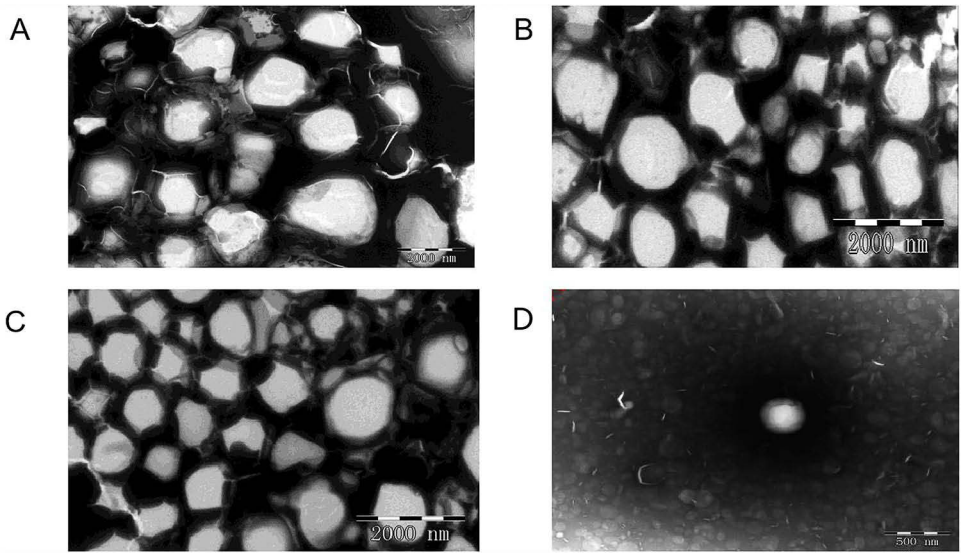

Figure 3 Transmission electron microscopy (TEM) images of 18β-glycyrrhetic acid liposomes: (**A**) A-18β-GA-L at ×2000 magnification, (**B**) B-18β-GA-L at ×2000 magnification, (**C**) C-18β-GA-L at ×2000 magnification, (**D**) D-18β-GA-L at ×7000 magnification.

In vitro Stability Analysis

The 18β-GA-Lips remained easily dispersible after being stored at 4°C for one month, with no significant changes in appearance. The Z-average size and EE of the liposomes exhibited minimal changes during storage (Tables S10–S11). Particle aggregation became apparent after one month of storage. These findings suggest that 18β-GA-Lips remained stable for up to 15 days.

In vivo Pharmacokinetic Analysis

The primary and secondary mass spectra of glycyrrhizinic acid and the internal standard (IS, lansoprazole) were obtained through mass spectrometric scanning, as illustrated in Figure S1 (A and B) and Figure S2 (A and B). The results showed that, at the lower limit of GA quantification, the measured and theoretical concentrations of glycyrrhizic acid in plasma containing the drug at low, medium, and high concentrations (2.00, 4.00, 80.00, and 1600.00 ng/mL) had an RSD value of less than 15%, and the RE value was in the range of −3.82% to 5.14%. This method meets the requirements of the methodology and can be used to determine the concentration of GA in rat plasma. The results are presented in Table 3.

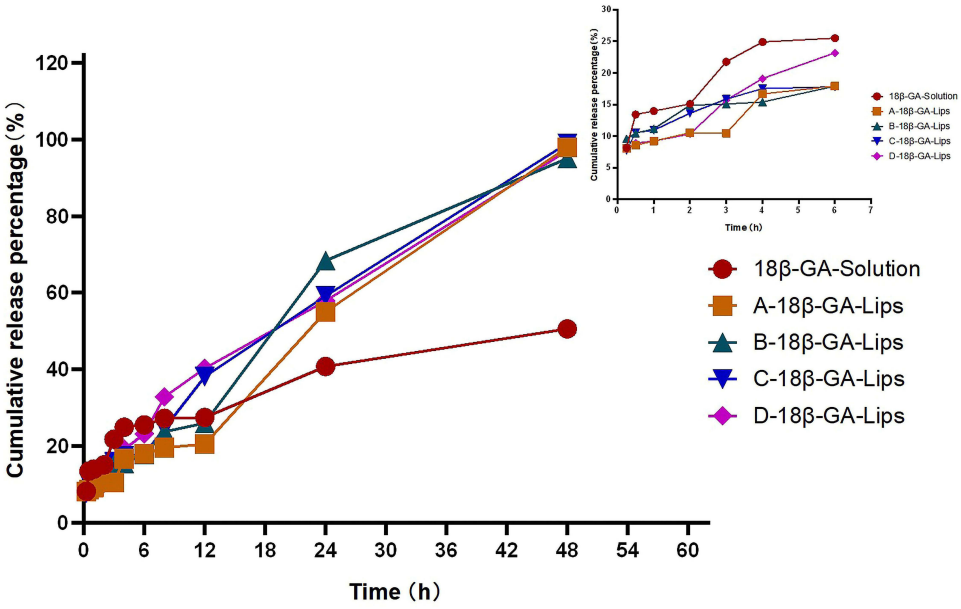

Figure 4 In vitro release profile of 18β-glycyrrhetic acid liposomes and 18β-GA solution (mean ± S.D., n = 6).

The plasma concentration profiles of A-18β-GA-Lips, B-18β-GA-Lips, C-18β-GA-Lips, D-18β-GA-Lips, and 18β-GA solution in SD rats over time are illustrated in Figure 5. At 0.25 and 0.5 hours, the plasma concentrations of the 18β-GA solution and 18β-GA-Lips reached their maximum levels and then gradually declined. The 18β-GA solution group exhibited rapid elimination after reaching its peak concentration, although traces of the drug were still detectable at 24 hours. The drug in the 18β-GA-Lips groups was eliminated slowly, with higher drug concentrations observed in the 18β-GA-Lips groups compared to the solution group at all time points following the peak. These findings indicate that 18β-GA-Lips significantly prolong drug retention time in rats, demonstrating a sustained-release effect in vivo.

The pharmacokinetic results are summarized in Table 4. The AUC $_{(0\rightarrow48)}$ values of 18β-GA-Lips in each group were 4.43, 3.27, 4.28, and 5.07 times higher than those of the solution group, indicating that the Formulation of 18β-GA into liposomes significantly enhanced its relative bioavailability. The MRT $_{(0\rightarrow48)}$ values of 18β-GA-Lips in each group were 2.10, 3.41, 1.73, and 1.46 times higher than those of the solution group, suggesting that liposomal formulation prolonged the average retention time of the drug in vivo. The $t_{1/2}$ values of 18β-GA lips for each group were 1.53, 1.32, 1.79, and 1.67 times higher than those of the solution group, confirming that the liposome-loaded 18β-GA achieved a slow-release effect. Additionally, there was no significant difference in Cmax and Tmax between the two formulations. The clearance of 18β-GA in liposomes for each group was only 1.15, 0.62, 0.96, and 0.90 times that of the solution group, respectively. Thus, liposomes not only achieved higher drug plasma levels and prolonged circulation time in rats but also effectively reduced the in vivo clearance rate.

Table 3 Precision and Accuracy of GA Samples (n = 6)

Marker Value (ng/mL)	Intra-assay (Intra-day)			Between batches (Inter-day)
	Measured Value Mean±S.D	RSD(%)	RE(%)	RSD(%)
2.00	1.99±0.25	13.80	−0.50	13.60
4.00	4.19±0.25	5.80	4.78	7.62
80.00	84.11±7.04	7.34	5.14	13.82
1600.00	1538.89±110.39	6.85	−3.82	9.23

https://doi.org/10.2147/DDDT.S547530

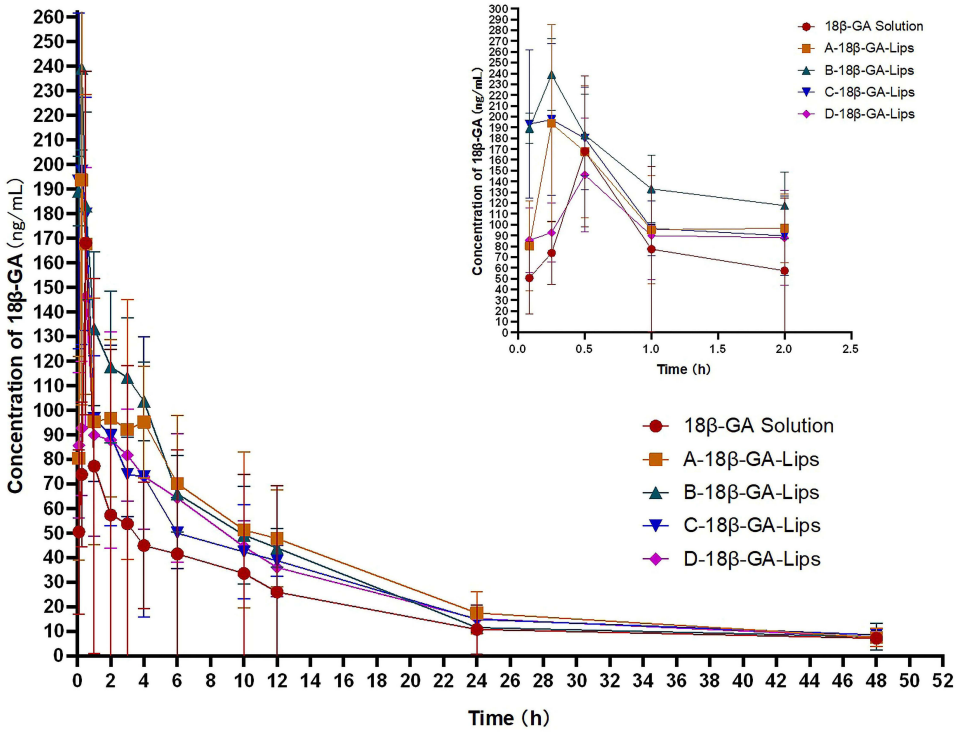

Figure 5 Plasma concentration–time curves for 18β-glycyrrhetic acid solution and 18β-GA liposomes in rats following aerosol inhalation (mean ± S.D., n = 6).

In vivo Biodistribution Analysis

Drug concentrations in the heart, liver, spleen, lungs, kidneys, and brain at different time points are illustrated in Figure 6A–6F. 18β-GA was primarily distributed in the lungs and liver. The drug concentrations in other organs were relatively low. Compared to the commercial 18β-GA solution, the concentration of 18β-GA-Lips in the lungs was significantly higher, likely due to macrophage uptake through the reticuloendothelial system. At all time points, the concentration of 18β-GA-Lips in the lungs consistently exceeded that of the 18β-GA solution. Furthermore, although the concentration decreased over time, it remained relatively high, indicating that the drug rapidly accumulated in the lungs and persisted for a prolonged period (Figure 6D). Specifically, the 18β-GA-Lips with a particle size of 800 nm (B-18β-GA-Lips) achieved the highest concentration and the longest retention time in the lung tissue of mice, indicating that 18β-GA-Lips with a particle size of 800 nm exhibit stronger lung-targeting ability compared to other 18β-GA-Lips and the 18β-GA solution.

The targeting parameters of lung tissue to drugs after atomized inhalation of 18β-GA-Lips in each group are summarized in Table 5. The Te values of lung tissue in A-18β-GA-Lips, C-18β-GA-Lips, and D-18β-GA-Lips were 48.33%, 34.40%, and 26.12%, respectively. These were not the highest values in the group, indicating that the lung tissue

Table 4 Pharmacokinetic Parameters of 18β-Glycyrrhetic Acid Solution and 18β-Glycyrrhetic Acid Liposomes (Mean ± S.D., n = 6)

Parameter / Groups	$AUC_{(0\rightarrow48)}$(μg/L*h)	$MRT_{(0\rightarrow48)}$ (h)	$t_{1/2}$(h)	Tmax (h)	Cmax (ng/L)
18β-GAsolution	441.00±342.76	10.72±0.80	7.67±1.33	0.42±0.36	188.47±167.59
A-18β-GA-Lips	1951.12±1106.03**	22.56±6.74*^^	11.79±4.14	0.26±0.10	217.6±112.00*
B-18β-GA-Lips	1443.90±754.06*	36.56±11.91$^{\#\#}$**	10.16±8.66	0.89±1.08	117.63±64.86$^{\#\#}$
C-18β-GA-Lips	1889.37±797.93**	18.62±4.39^^	13.74±5.33	0.30±0.14	181.8±71.86$^{\#}$
D-18β-GA-Lips	2240.81±806.14**	15.69±4.67^^	12.88±5.33	0.72±1.71	171.88±30.69$^{\#\#}$

Notes: *, $P<0.05$; **, $P<0.01$ vs 18β-GAsolution; #, $P<0.05$; ##, $P<0.01$ vs A-18β-GA-Lips; ^^, $P<0.01$ vs B-18β-GA-Lips.

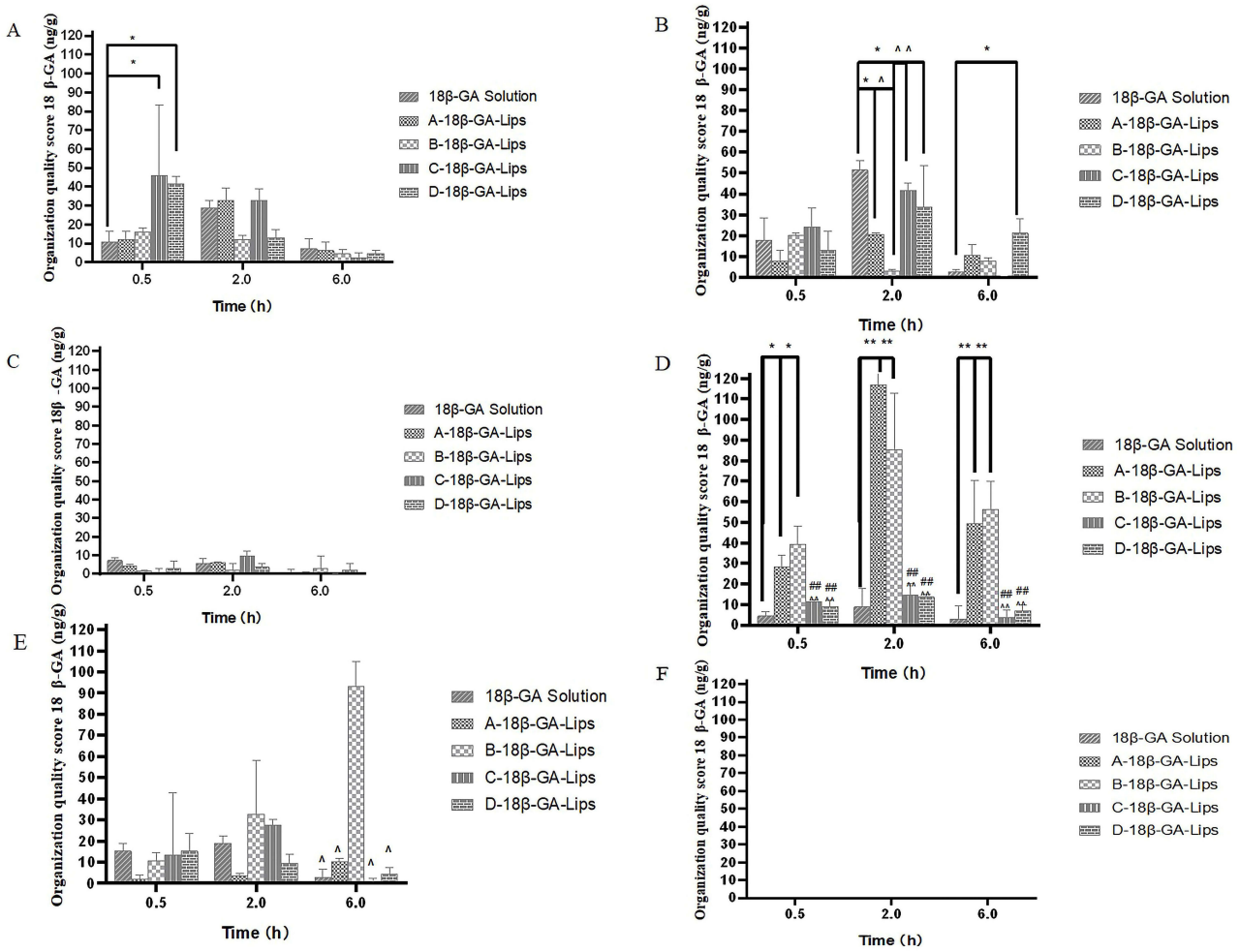

Figure 6 Quality scores of 18β-glycyrrhetic acid solution and 18β-GA liposomes in mice following aerosol inhalation (mean ± S.D., n = 5). (**A**) Heart, (**B**) Liver, (**C**) Spleen, (**D**) Lung, (**E**) Kidney, (**F**) Brain. *P< 0.05; **P < 0.01 vs 18β-GA Solution; $^{\#\#}P$ < 0.01 vs A-18β-GA-Lips; ^P < 0.05; ^^P < 0.01 vs B-18β-GA-Lips.

targeting efficiency in these formulations was lower compared to other organ tissues. The Te value of lung tissue in B-18β-GA-Lips was 54.13%, which was the highest in the group, indicating that the lung tissue in this formulation exhibited the greatest targeting efficiency compared to other organ tissues.

Subacute Inhalation Toxicity of 18β-GA-Lips

Observation of Clinical Symptoms in Rats

During the 18β-GA-Lips atomization administration, clinical observations of animals in each experimental group revealed no signs of panic, convulsions, ataxic gait, or other abnormalities. The rats maintained a normal diet and defecation, were responsive to stimulation, and exhibited no irregularities in stool properties, skin and mucosa,

Table 5 Lung Targeting Parameters of 18β-GA -Lips in Different Experimental Groups

Groups	Te (%)	RTe	Re	Ce
A-18β-GA-Lips	48.33	2.72	4.48	13.07
B-18β-GA-Lips	54.13	3.06	6.55	9.55
C-18β-GA-Lips	34.30	1.94	1.77	1.64
D-18β-GA-Lips	26.12	1.47	1.15	1.54

https://doi.org/10.2147/DDDT.S547530

respiration, heartbeat, fur, eyes, nose, or limbs. During the experiment, three rats in the high-dose group (100 mg/kg, 14 days), one rat in the low-dose group (25 mg/kg, 14 days), and five rats in the high-dose group (100 mg/kg, 21 days) died, all due to tracheal obstruction and suffocation during administration.

Results of Weight Changes in Rats

During the experiment, the weight of rats in each group steadily increased, with minimal differences observed between groups. No significant differences in weight were found when compared to the same-period and same-sex control group. Weight changes at various time points exhibited irregular fluctuations and no dose–response relationship, suggesting that the observed weight changes were not biologically significant (Table S12).

Results of Food Intake Changes in Rats

During the administration period, food intake differences between each dose group of rats and the corresponding same-period, same-sex control group were minimal, with no statistically significant differences observed. Changes in food intake exhibited irregular fluctuations and showed no dose–response relationship. These findings suggest that the changes in food intake have no biological significance (Tables S13 and S14).

Results of Functional Observation Combination Test

During the administration period, functional observation combination tests were performed weekly for each dose group of rats. Among the 23 indicators assessed, no continuous or consistent trends were observed. All indicators exhibited irregular fluctuations and no dose–response relationship, suggesting that these changes were not biologically significant (Table S15).

Results of Blood Index Analysis in Rats

As shown in Tables S16 and S17, after 21 days of atomization with 18β-GA-Lips, the MCV and MCH values in the high-dose group (100 mg/kg) were significantly lower than those in the control group at the same time ($P < 0.05$). After 14 days of aerosol administration of 18β-GA-Lips, the RBC, HGB, and MCHC values in the high-dose group (100 mg/kg) increased ($P < 0.05$), while the MCV, MCH, and RDWCV values decreased ($P < 0.05$) compared to the control group during the same period. In the low-dose group (25 mg/kg), RBC, MCHC, and RDWCV values increased ($P < 0.05$), while MCV and MCH values decreased ($P < 0.05$). However, these changes were within the normal reference range for SD rats in our laboratory and exhibited no dose-dependent relationship, indicating no significant toxicological relevance. No other indicators exhibited abnormal changes of toxicological significance.

Results of Biochemical Indicators in Rats

As shown in Tables S18, after 21 days of 18β-GA-Lips atomization, the TP, GLB, and LDH values in the high-dose group (100 mg/kg) significantly increased ($P < 0.05$), while the T–BIL, IBIL, ALP, CRE, GLU, and TBA values decreased ($P < 0.05$). Compared to the control group during the same period, the D-BIL and LDH values in the high-dose group (100 mg/kg) increased ($P < 0.05$) 14 days after atomization of 18β-GA-Lips, while the ALP value decreased ($P < 0.05$). In the low-dose group (25 mg/kg), LDH values increased ($P < 0.05$), while T–BIL, IBIL, ALP, CRE, TCHO, HDL-C, LDL-C, and CK values decreased ($P < 0.05$). However, these changes were within the normal reference range for SD rats in our laboratory and exhibited no dose-dependent relationship, indicating no significant toxicological relevance. No other indicators exhibited abnormal changes with toxicological significance.

Results of Urine Indicators in Rats

As shown in Table S18, after 21 days of high-dose (100 mg/kg) atomized administration of 18β-GA-Lips, ketone bodies increased in three rats. In the low-dose group (25 mg/kg), one rat exhibited slight urinary protein. However, these changes were dose-dependent and not biologically significant. No other indicators showed abnormal changes with toxicological relevance.

Results of Ultrasound Analysis in Rats

As shown in Tables S19 and S20, after 21 days of atomization administration of 18β-GA-Lips, the SV value in the high-dose group was significantly higher than that in the control group during the same period ($P < 0.05$). As shown in Tables S19 and S20, after 21 days of atomization administration of 18β-GA-Lips, the SV value in the high-dose group was significantly higher than

that in the control group during the same period ($P < 0.05$). In the low-dose group (25 mg/kg), LV Mass and LV Mass Cor values decreased significantly ($P < 0.05$). However, these changes were within the normal reference range for SD rats in our laboratory and exhibited no dose-dependent relationship, indicating no significant toxicological relevance. No other indicators exhibited abnormal changes of toxicological significance.

Results of Histopathological Examination in Rats

Throughout the experiment, three rats in the high-dose group (100 mg/kg, 14 days) died of asphyxia due to tracheal blockage during drug atomization, one rat in the low-dose group (25 mg/kg, 14 days), and five rats in the high-dose group (100 mg/kg, 21 days). Autopsies of the deceased animals revealed no significant abnormalities.

Histopathological Observation: After the experiment, tissue samples from the heart, liver, spleen, lungs, kidneys, brain, intestine, muscle, spinal cord, trachea, skin, and uterus/testes were collected, sectioned, stained with H&E, and examined histopathologically. Compared to the normal group, the tissue structures of all organs appeared normal, with no obvious lesions observed, indicating no pathological significance. Details are provided in Figures S3 and S4.

Effects of 18β-GA Solutions, 18β-GA-Lips on Echocardiography of SuHx-Induced PAH

The echocardiographic results indicated that the velocity profile shape of rats in the SuHx group changed from the "round" profile observed in the control group (Figure 7A) to the characteristic "dome and peak" profile of PAH (Figure 7B). However, when rats in the SuHx group were treated with 18β-GA solutions (6.25 and 100 mg/kg), 18β-GA-Lips (6.25 and 50 mg/kg), and NO (Figure 7C–G), the abnormal changes were significantly improved. Compared with the control group, the echocardiographic parameters, PAAT and PVmax, in the SuHx group were significantly reduced, and RVESD was significantly increased ($P < 0.01$ and $P < 0.05$, respectively; Figure 8). However, after administration of 18β-GA solutions (6.25 and 100 mg/kg) and 18β-GA-Lips (6.25 and 50 mg/kg) along with NO treatment, the echocardiographic parameters PAAT and PVmax in rats significantly increased, while RVESD significantly decreased ($P < 0.01$ and $P < 0.05$, respectively; Figure 8). These findings suggest that 18β-GA treatment improved the PAH induced by SuHx in rats. No significant difference was observed between the treatment groups.

Effects of 18β-GA Solutions and 18β-GA-Lips on Hemodynamic Measurements in SuHx-Induced PAH

We evaluated the protective effects of 18β-GA solutions and 18β-GA-Lips (18β-GA-Lips) on SuHx-induced PAH by measuring mPAP and RVSP levels. Six weeks after SuHx administration, mPAP and RVSP levels significantly increased in the SuHx group compared to the control group ($P < 0.01$; Figures 9 and 10), confirming the successful establishment of the SuHx-induced rat model. Treatment interventions with 18β-GA solutions, 18β-GA-Lips, and NO were initiated three weeks after SuHx exposure. Rats treated with 18β-GA solutions (6.25 and 100 mg/kg), 18β-GA-Lips (6.25 and 50 mg/kg), and NO exhibited significantly lower mPAP and RVSP levels compared to the SuHx group ($P < 0.01$; Figures 9 and 10). These findings indicate that oral and nebulized 18β-GA solutions and atomized 18β-GA-Lips can alleviate SuHx-induced PAH in rats. No statistical differences were observed between the administration groups.

Effects of 18β-GA Solutions and 18β-GA-Lips on Right Heart Hypertrophy in SuHx-Induced PAH

The weight ratio of RV/(LV+S) was calculated to assess the right ventricular hypertrophy index (RVHI). A significant increase in RVHI was observed as a result of elevated pulmonary arterial pressure. This further confirms that subcutaneous injection of Su5416 combined with hypoxia induces severe PAH. In the SuHx group, RVHI was significantly elevated ($P < 0.01$; Figure 11). Compared to RVHI in the SuHx group, RVHI was markedly reduced by oral and nebulized 18β-GA solutions, atomized 18β-GA-Lips, and NO ($P < 0.01$; Figure 11). Among them, compared with atomized 18β-GA solutions (6.25 mg/kg), the two doses of atomized 18β-GA-Lips (6.25 mg/kg and 50 mg/kg) showed a significant reduction ($P < 0.01$ and $P < 0.05$, respectively; Figure 11), while compared with oral 18β-GA solutions, only atomized 18β-GA-Lips (50 mg/kg) had a difference ($P < 0.05$, Figure 11). As expected, 18β-GA-Lips obviously alleviated SuHx -induced RVHI better.

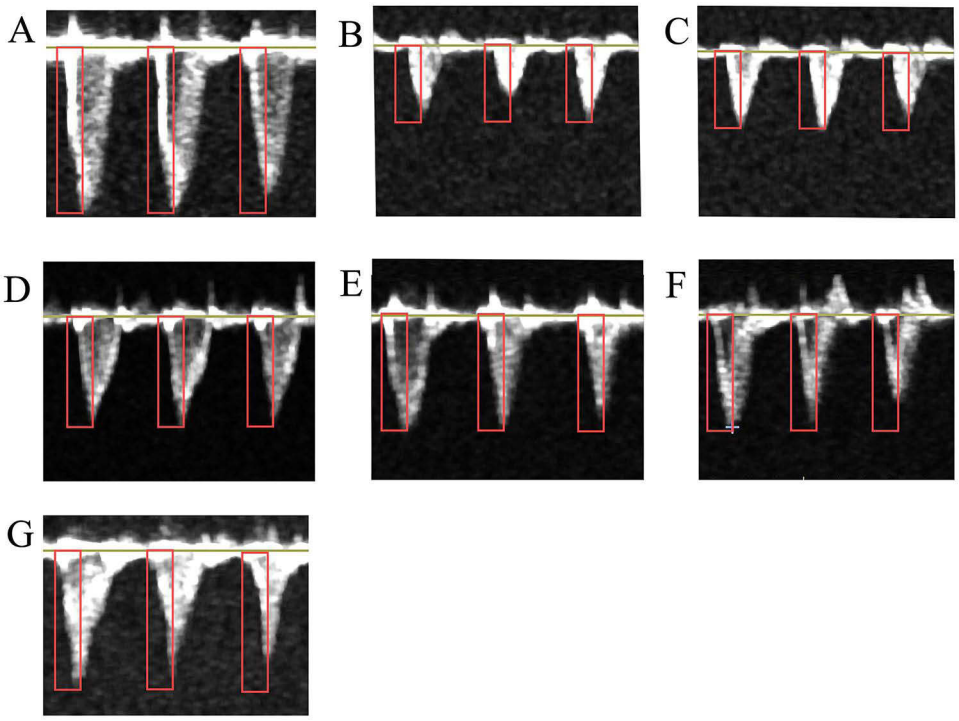

Figure 7 Effect of 18β-glycyrrhetic acid solution (18β-GA-S) and 18β-GA liposomes (18β-GA-L) on echocardiographic velocity profile morphology. Data are presented as mean ± SEM (n = 6). (**A**) Control group; (**B**) SuHx group; (**C**) 18β-GA-S 6.25 mg/kg group; (**D**) 18β-GA-L 6.25 mg/kg group; (**E**) 18β-GA-L 50 mg/kg group; (**F**) 18β-GA-S 100 mg/kg group; (**G**) NO group.
Abbreviations: SuHx, Su5416 + hypoxia; 18β-GA-S (6.25 mg/kg), SuHx + atomized 18β-Glycyrrhetic Acid Solution; 18β-GA-L (6.25 mg/kg and 50 mg/kg), SuHx + atomized 18β-Glycyrrhetic Acid Liposome; 18β-GA-S (100 mg/kg), SuHx + intragastric 18β-Glycyrrhetic Acid Solution.

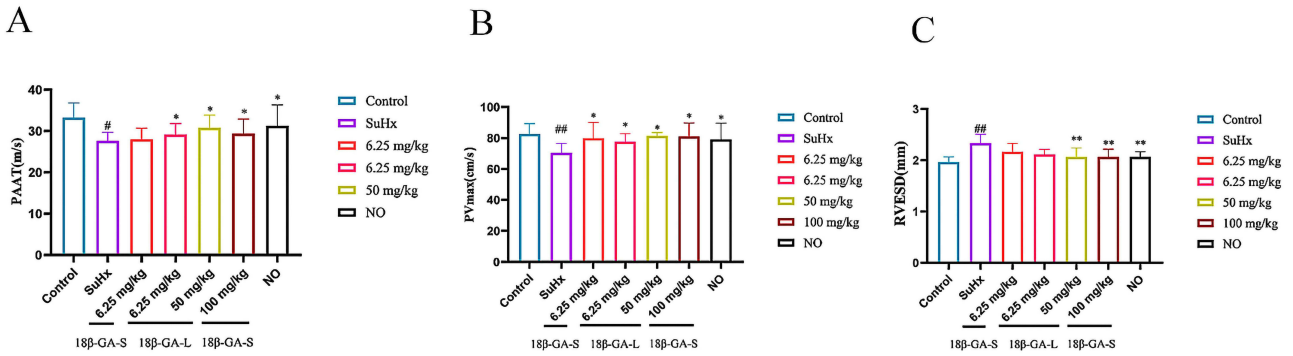

Figure 8 Effect of 18β-glycyrrhetic acid solution (18β-GA-S) and 18β-GA liposomes (18β-GA-L) on echocardiographic parameters. Data are expressed as mean ± SEM (n = 6). (**A**) Effect of 18β-GA-S and 18β-GA-L on pulmonary acceleration time (PAAT); (**B**) Effect of 18β-GA-S and 18β-GA-L on maximum pulmonary blood flow velocity (PVmax); (**C**) Effect of 18β-GA-S and 18β-GA-L on end systolic diameter of the right ventricle (RVESD). $^{\#}P < 0.05$, $^{\#\#}P < 0.01$ vs control group; $^{*}P < 0.05$, $^{**}P < 0.01$ vs SuHx group.
Abbreviations: SuHx, Su5416 + hypoxia; 18β-GA-S (6.25 mg/kg), SuHx + atomized 18β-Glycyrrhetic Acid Solution; 18β-GA-L (6.25 mg/kg and 50 mg/kg), SuHx + atomized 18β-Glycyrrhetic Acid Liposome; 18β-GA-S (100 mg/kg), SuHx + intragastric 18β-Glycyrrhetic Acid Solution. PAAT, pulmonary acceleration time; PVmax, maximum pulmonary blood flow velocity; RVESD, end systolic diameter of right ventricle.

Effects of 18β-GA Solution and 18β-GA-Lips on Pulmonary Vascular Remodeling in SuHx-Induced PAH

H&E Staining

H&E staining was performed to evaluate the pathological changes in the small pulmonary arteries. H&E staining revealed that, compared with the lung histology of the control group, the SuHx group exhibited thickening of the pulmonary artery

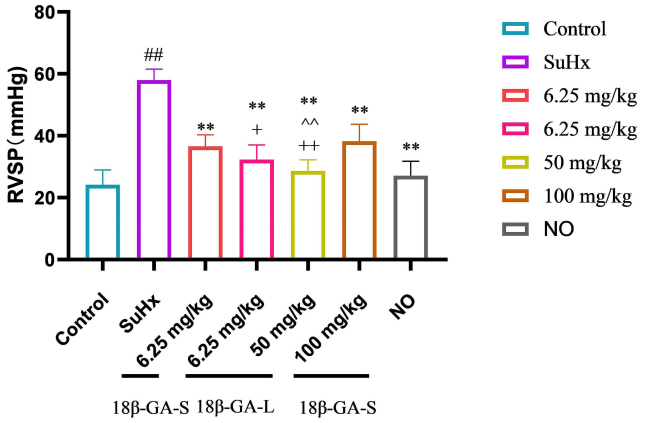

Figure 9 Effect of 18β-glycyrrhetic acid solution (18β-GA-S) and 18β-GA liposomes (18β-GA-L) on right ventricular systolic pressure (RVSP). Data are presented as mean ± SEM (n = 6). $^{\#\#}P < 0.01$ vs control group, $^{**}P < 0.01$ vs SuHx group, $^{\wedge}P < 0.05$, $^{\wedge\wedge}P < 0.01$ vs 18β-GA-S (6.25 mg/kg), $^{+}P < 0.05$, $^{++}P < 0.01$ vs 18β-GA-S (100 mg/kg).
Abbreviations: SuHx, Su5416 + hypoxia; 18β-GA-S (6.25 mg/kg), SuHx + atomized 18β-Glycyrrhetic Acid Solution; 18β-GA-L (6.25 mg/kg and 50 mg/kg), SuHx + atomized 18β-Glycyrrhetic Acid Liposome; 18β-GA-S (100 mg/kg), SuHx + intragastric 18β-Glycyrrhetic Acid Solution; RVSP, right ventricular systolic pressure.

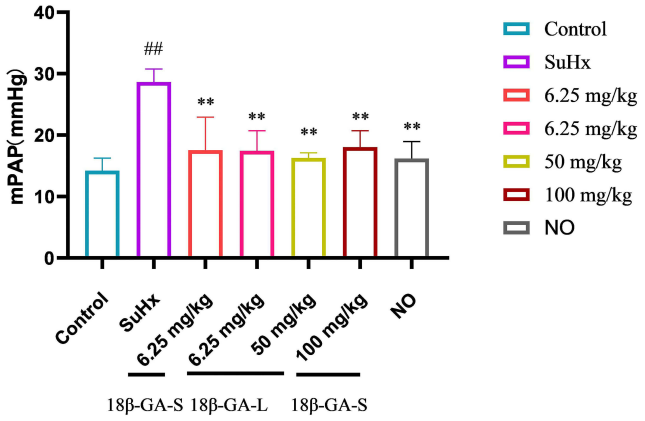

Figure 10 Effect of 18β-glycyrrhetic acid solution (18β-GA-S) and 18β-GA liposomes (18β-GA-L) on mean pulmonary arterial pressure (mPAP). Data are expressed as mean ± SEM (n = 6). $^{\#\#}P < 0.01$ vs control group, $^{**}P < 0.01$ vs SuHx group.
Abbreviations: SuHx, Su5416 + hypoxia; 18β-GA-S (6.25 mg/kg), SuHx + atomized 18β-Glycyrrhetic Acid Solution; 18β-GA-L (6.25 mg/kg and 50 mg/kg), SuHx + atomized 18β-Glycyrrhetic Acid Liposome; 18β-GA-S (100 mg/kg), SuHx + intragastric 18β-Glycyrrhetic Acid Solution; mPAP, mean pulmonary arterial pressure.

wall and severe stenosis of the lumen (Figure 12). Following treatment with 18β-GA solutions, 18β-GA-Lips, and NO, significant improvements in pulmonary arterial morphology were observed. Additionally, WT% and WA% were measured to assess the effects of 18β-GA solutions and 18β-GA-Lips on pulmonary vascular remodeling. WT% and WA% were significantly increased in the SuHx-treated group compared with the control group ($P < 0.01$; Figure 13A and B). In the 18β-GA solutions, 18β-GA-Lips, and NO groups, WT% and WA% were significantly reduced compared with the SuHx group ($P < 0.01$; Figure 13A and B). Among the groups, WT% and WA% were significantly reduced in the two doses of atomized 18β-GA-Lips (6.25 mg/kg and 50 mg/kg) compared with atomized 18β-GA solutions (6.25 mg/kg) ($P < 0.01$ and $P < 0.05$, respectively; Figure 13). In contrast, WT% and WA% were significantly different between the two doses of atomized 18β-GA-Lips (6.25 mg/kg and 50 mg/kg) and oral 18β-GA solutions ($P < 0.01$; Figure 13). As expected, 18β-GA-Lips significantly alleviated SuHx-induced pulmonary vascular remodeling.

Transmission Electron Microscopy (TEM) Analysis

Pulmonary artery ultrastructure was analyzed using transmission electron microscopy. Under the electron microscope, the structure of mitochondria, connective tissue, and smooth muscle cells in the pulmonary vessels of rats in the control group appeared normal (Figure 14A). In the SuHx group, the mitochondrial structure was abnormal, vasoconstriction was present, the number of smooth muscle cells in the vascular wall increased, and edema was observed around the

https://doi.org/10.2147/DDDT.S547530

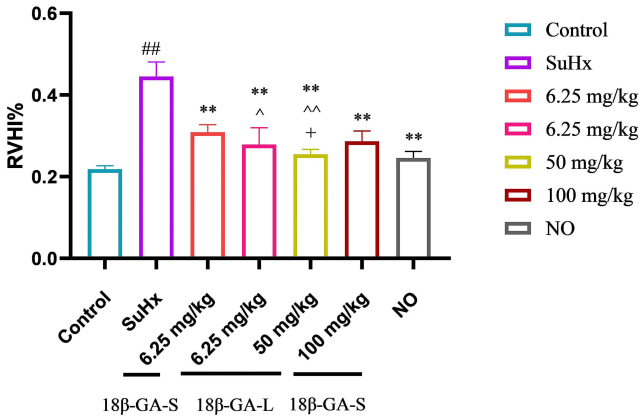

Figure 11 Effect of 18β-glycyrrhetic acid solution (18β-GA-S) and 18β-GA liposomes (18β-GA-L) on Right Ventricular Hypertrophy Index (RVHI). Data are presented as mean ± SEM (n = 6). $^{\#\#}P < 0.01$ vs control group, $^{**}P < 0.01$ vs SuHx group, $^{\wedge\wedge}P < 0.01$ vs 18β-GA-S (6.25 mg/kg); $^{+}P < 0.05$, $^{++}P < 0.01$ vs 18β-GA-S (100 mg/kg).
Abbreviations: SuHx, Su5416 + hypoxia; 18β-GA-S (6.25 mg/kg), SuHx + atomized 18β-Glycyrrhetic Acid Solution; 18β-GA-L (6.25 mg/kg and 50 mg/kg), SuHx + atomized 18β-Glycyrrhetic Acid Liposome; 18β-GA-S (100 mg/kg), SuHx + intragastric 18β-Glycyrrhetic Acid Solution; RVHI, right ventricular hypertrophy index.

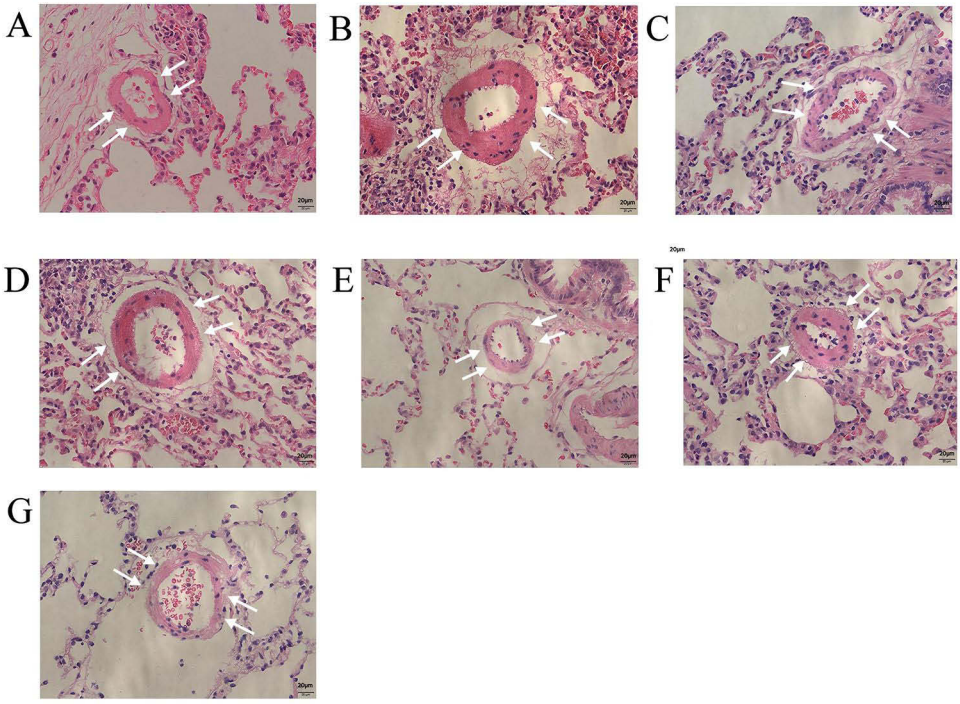

Figure 12 Effect of 18β-glycyrrhetic acid solution (18β-GA-S) and 18β-GA liposomes (18β-GA-L) on pulmonary vascular remodeling. Data are expressed as mean ± SEM (n = 6). (**A**) Control group; (**B**) SuHx group; (**C**) 18β-GA-S 6.25 mg/kg group; (**D**) 18β-GA-L 6.25 mg/kg group; (**E**) 18β-GA-L 50 mg/kg group; (**F**) 18β-GA-S 100 mg/kg group; (**G**) NO group.
Abbreviations: SuHx, Su5416 + hypoxia; 18β-GA-S (6.25 mg/kg), SuHx + atomized 18β-Glycyrrhetic Acid Solution; 18β-GA-L (6.25 mg/kg and 50 mg/kg), SuHx + atomized 18β-Glycyrrhetic Acid Liposome; 18β-GA-S (100 mg/kg), SuHx + intragastric 18β-Glycyrrhetic Acid Solution.

capillaries (Figure 14B). After treatment with 18β-GA solutions, 18β-GA-Lips, and NO, the mitochondrial structure in rats improved, smooth muscle cells in the capillary wall were reduced, and the capillary lumen appeared more normal (Figure 14C–G). These results suggest that the histopathological characteristics of lung tissue in the 18β-GA solutions and 18β-GA-Lips treated rats were alleviated.

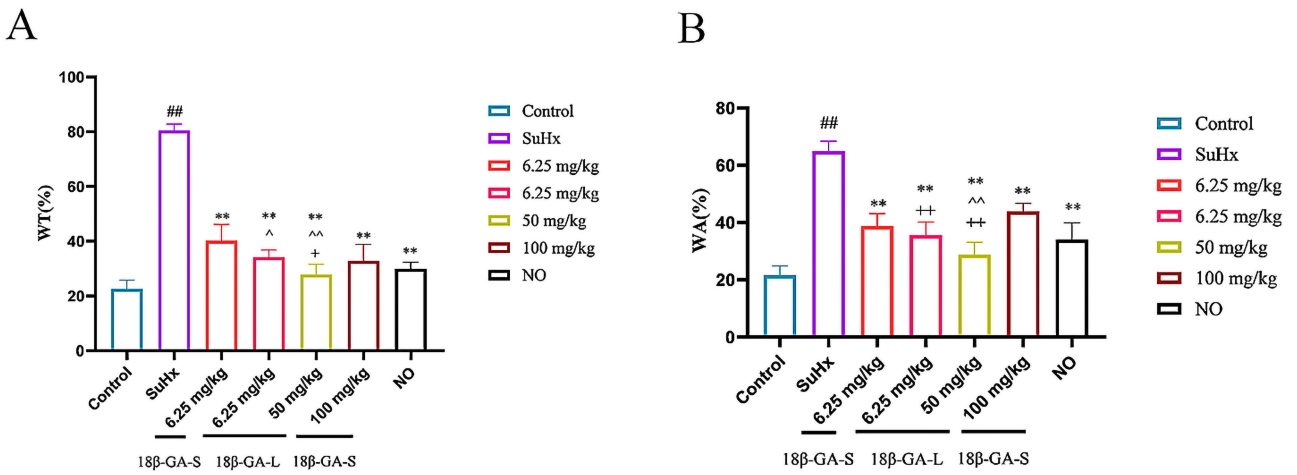

Figure 13 Effect of 18β-glycyrrhetic acid solution (18β-GA-S) and 18β-GA liposomes (18β-GA-L) on the ratio of vascular wall thickness (WT%) (**A**); Effect of 18β-GA-S and 18β-GA-L on the ratio of vascular wall area (WA%) (**B**). Data are expressed as mean ± SEM (n = 6). $^{\#\#}P < 0.01$ vs control group; $^{**}P < 0.01$ vs SuHx group; $^{\wedge}P < 0.05$, $^{\wedge\wedge}P < 0.01$ vs 18β-GA-S (6.25 mg/kg); $^{+}P < 0.05$, $^{++}P < 0.01$ vs 18β-GA-S (100 mg/kg).

Abbreviations: SuHx, Su5416 + hypoxia; 18β-GA-S (6.25 mg/kg), SuHx + atomized 18β-Glycyrrhetic Acid Solution; 18β-GA-L (6.25 mg/kg and 50 mg/kg), SuHx + atomized 18β-Glycyrrhetic Acid Liposome; 18β-GA-S (100 mg/kg), SuHx + intragastric 18β-Glycyrrhetic Acid Solution. WT%, ratio of vascular wall thickness; WA%, ratio of vascular wall area.

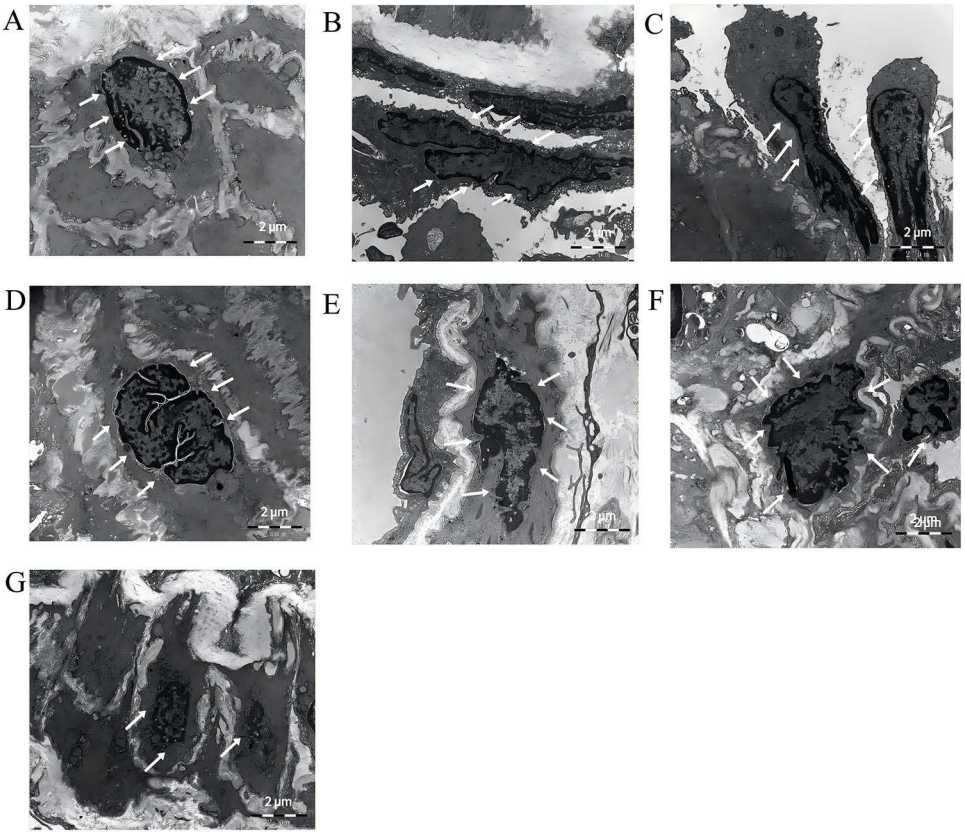

Figure 14 Ultrathin cross-sections of pulmonary vessels in rats examined under transmission electron microscopy (TEM) at 12,000× magnification (Scale bar = 2,000 nm). (**A**) Control group; (**B**) SuHx group; (**C**) 18β-GA-S 6.25 mg/kg group; (**D**) 18β-GA-L 6.25 mg/kg group; (**E**) 18β-GA-L 50 mg/kg group; (**F**) 18β-GA-S 100 mg/kg group; (**G**) NO group.

https://doi.org/10.2147/DDDT.S547530

Discussion

In the present study, we explored liposomes that could be engineered to target the lungs by controlling particle size, aiming to effectively treat PAH. Our research group has previously confirmed that 18β-GA can effectively treat pulmonary hypertension.[16,17] However, because 18β-GA is poorly soluble in water, the oral effective dose for rats is large, and long-term high-dose administration has been shown to cause dose-dependent side effects, such as sodium retention and potassium loss.[18,19] In this study, we developed 18β-GA liposomes to enhance local drug concentration and improve the effectiveness of 18β-GA intervention via nebulization inhalation. Selecting the appropriate particle size for accurate lung targeting has been one of the challenges in their Formulation. From the preliminary experiments, we found that different molar ratios of excipients result in variations in the particle sizes of the prepared liposomes. Based on single-factor experimental analysis, three molar ratio groups were selected. The role of phospholipids is to enhance the toughness of the membrane material.[28] As the amount of phospholipid increases, the membrane material becomes stronger, leading to liposome aggregation and an increase in particle size. DSPE-MPEG2000 is commonly used in targeted drug delivery systems and enhances liposome stability.[29] To prepare liposomes with smaller particle sizes, the thin-film dispersion probe ultrasound method was selected. The desired conditions can only be achieved when the appropriate ultrasonic time and power are determined. Insufficient ultrasonic time or low power is inadequate to uniformly reduce large particles to smaller sizes. If the ultrasonic time is too long or the power is too high, the vesicles may be damaged. Additionally, if the ultrasonic time is too long, the temperature generated by the ultrasonic probe will increase, reaching the phase transition temperature and resulting in liposome damage and an uneven particle size distribution.

The size of the liposomes observed using TEM was smaller than that observed with the nanoparticle size, Zeta potential, and molecular weight analyzer; however, the size difference was not significant, which may be attributed to the negligible effect of salvation in the case of liposomes.[30] Based on the four groups (A-18β-GA-Lips, B-18β-GA-Lips, C-18β-GA-Lips, and D-18β-GA-Lips) used in the previous screening, the morphology, particle size, potential, PDI, encapsulation efficiency, and drug loading were assessed, all of which exhibited good physical and chemical properties.

In the in vitro drug release study, attention was focused on the release duration in a specific medium that mimicked the lung emptying time. The results clearly indicate slow release and increased solubility of 18β-GA-Lips. This may be due to the liposome surface being coated with the amphoteric substance DSPE-MPEG2000, with a hydrophilic exterior that partially prevents the diffusion of 18β-GA into the release medium, thereby ensuring the drug's prolonged activity after entering the human body.[31,32] Stability studies clearly indicate that the developed liposomes remained stable in terms of size and EE% for 15 days at 4 ± 2°C. In conclusion, in vivo pharmacokinetics and tissue targeting are of greater importance.

In the pharmacokinetics study, the $AUC_{(0–48\ h)}$ of all liposomal formulations was much greater than that of the 18β-GA solution, indicating greater bioavailability of 18β-GA in liposomal form. This was further supported by the higher $MRT_{(0→48)}$ values observed with liposomes compared to those observed with the plain drug. This may be due to liposome encapsulation of drugs, or because DSPE-MPEG2000 has a polar long chain, which increases the steric hindrance of liposomes, reduces the probability of phagocytosis by phagocytes, and prolongs the residence time of drugs in the blood.[31,33] Although there was no significant difference between the 18β-GA solution group and all 18β-GA liposome groups in terms of $t_{1/2}$, the $t_{1/2}$ for each liposome group was prolonged, and the slow-release effect was observed.

In the tissue distribution study, all liposomes showed a high concentration of the drug in the lung at all three time points (0.5, 2, and 6 h), indicating that more drug was available from the liposomes in the systemic circulation for easier access to the lung. The 18β-GA concentration in the lung followed the order: A-18β-GA-lips > B-18β-GA-lips > C-18β-GA-lips > D-18β-GA-lips > 18β-GA solution. This may be due to the large absorption area in the lung and the thin barrier between the circulating blood and lung tissue after the drug is administered via the lungs.[33] Liposomes with suitable particle sizes slowly release the encapsulated drug in the lungs over an extended period, exhibiting long distribution times and high concentrations in lung tissues. Therefore, all 18β-GA-lips demonstrated good targeted drug delivery system behavior, while liposomes with smaller particle sizes reached other tissues through the capillaries around

the alveoli, exerting a slow-release effect in the heart and liver.[34,35] Lung tissue targeting of 18β-GA-lips with different particle sizes was assessed by calculating the targeting parameters from pharmacokinetic data. Te reflects the Formulation's selectivity for the target tissue.[31,36] The Te value in the lung for A-18β-GA-Lips was 48.33%, and for B-18β-GA-Lips, it was 54.13%. C-18β-GA-Lips reduced lung targeting and increased selectivity for the spleen, while D-18β-GA-Lips also decreased lung targeting. When the passive targeting formulation is atomized, particle size determines its distribution in vivo. When the particle size ranges from 500 to 5000 nm, it is retained in lung tissue for an extended period, while particles smaller than 500 nm are primarily distributed to organs with abundant endoplasmic reticulum, such as the liver and spleen, demonstrating passive targeting.[13,36,37] In this experiment, it was found that when 18β-GA was encapsulated in liposomes with a particle size greater than 500 nm, lung selectivity was significantly enhanced compared to other tissues. The RTE value reflects the degree of improvement in the targeting efficiency of the Formulation to the target tissue. The results showed that targeting of all 18β-GA-Lips formulations to lung tissue increased by 2.72, 3.06, 1.94, and 1.47 times, indicating significant lung targeting, particularly in the B-18β-GA-Lips group. An RTE value greater than 1 indicates that the drug formulation targets specific tissues. A-18β-GA-Lips and B-18β-GA-Lips had the highest RTE values in lung tissue (4.48 and 6.55), while C-18β-GA-Lips and D-18β-GA-Lips exhibited higher RTE values in spleen tissue than in lung tissue. The results showed that the distribution of 18β-GA in the lung could be significantly enhanced by the atomized inhalation of liposomes with an appropriate particle size. The Ce value indicates the extent to which the Formulation alters the drug distribution within the tissue. A-18β-GA-Lips, B-18β-GA-Lips, and D-18β-GA-Lips exhibited the highest Ce values in lung tissue (13.07, 9.55, and 1.54). This further verifies that A-18β-GA-Lips and B-18β-GA-Lips exhibit lung targeting.

In this experiment, we explored the ability of liposomes with different particle sizes to target the lungs, aiming to prepare 18β-GA liposomes with passive lung targeting and high encapsulation efficiency.

Subacute toxicity tests were conducted on 18β-GA-Lips to investigate the toxic effects caused by repeated exposure to high doses. The experiment primarily analyzed body weight, food intake, general clinical manifestations, FOB, blood routine, biochemical markers, urine routine, and other indicators in the test animals. Although some indicators showed statistical significance compared to the same-sex control group, these changes were within the normal reference range for the test mice in our laboratory, and no dose-dependent relationship was observed, indicating no significant toxicological effect. No abnormalities were observed in the histopathological examination. In summary, under the conditions of this experiment, 18β-GA-Lips did not exhibit any obvious toxic effects on the rats.

Based on the EE%, DL%, stability, pharmacokinetic data, tissue distribution characteristics, and lung targeting of all liposomes, B-18β-GA-Lips was selected to evaluate its therapeutic effect on PAH.

A previous study by our research group found that intragastric administration of 18β-GA (100 mg/kg) had a significant therapeutic effect on rats with PAH. This study is the first to demonstrate the therapeutic effect of 18β-GA on PAH.[16,17] Building upon previous studies, this research first applied Su5416 combined with hypoxia to establish a PAH rat model. After 21 days of model establishment, 18β-GA-solutions and B-18β-GA-Lips were administered for 21 consecutive days to evaluate the effect of 18β-GA on PAH. The results showed that mPAP and RVSP were significantly increased in the SuHx group, and the degree of lumen stenosis was high. Following administration of 18β-GA-solutions and 18β-GA-Lips, mPAP and RVSP in rats from all treatment groups decreased, and the degree of lumen stenosis was reduced. Among these, nebulized administration of 18β-GA-Lips (50 mg/kg) demonstrated a more pronounced therapeutic effect. The results are consistent with previous studies on the effects of 18β-GA and isorhamnetin in MCT-induced PAH rat models, suggesting that our findings exhibit high reproducibility and hold promise for clinical application.[16,17,38]

The SuHx-induced PAH rat model is commonly used to simulate the pathological characteristics of human PAH. The hormone levels in male rats are stable, reducing the influence of the reproductive cycle on drug efficacy, and making the procedure more convenient. Thus, it is frequently used in preclinical studies.[39,40] SU5416 is an inhibitor of the vascular endothelial growth factor receptor (VEGFR), which causes endothelial cell dysfunction and contributes to the pathogenesis of pulmonary hypertension. In combination with hypoxia, SU5416 induces complex occlusive vascular remodeling specific to pulmonary hypertension, resembling the condition observed in humans.[41–43] Therefore, we selected the SuHx-induced PAH model for our study.

18β-GA is a chemical constituent of licorice. The protective effect of 18β-GA on the lungs has been a focal point of research, including its impact on lung fibrosis, pneumonia, asthma, pulmonary hypertension, and other related diseases. We administered 18β-GA using various methods and drug delivery systems after subcutaneous injection of SuHx and hypoxia for 21 days, and observed hemodynamic indices, among others. The 18β-GA dose in rats was selected based on the varying bioavailability of 18β-GA via both oral and aerosol inhalation routes. Therefore, to achieve the same oral bioavailability as observed with aerosol inhalation, the aerosol inhalation dose is approximately 25% of the oral dose. We selected the low dose of 18β-GA administered intragastrically as the corresponding low dose for atomized inhalation, which was adjusted to 6.25 mg/kg. To compare whether atomized inhalation offers distinct advantages, we included a 100 mg/kg intragastric administration group for comparison. To observe whether liposomes offer advantages in treating PAH through atomized inhalation compared to a simple solution, an atomized 18β-GA solution group was established. All these factors suggest that 18β-GA may exhibit a pharmacological response depending on the dose range and mode of administration, which could be attributed to its highly variable bioavailability, resulting in inconsistent therapeutic effects.

The continuous increase in pulmonary vascular resistance and pressure in PAH patients and animal models results in abnormal hemodynamic parameters, including elevated mPAP and RVSP, which in turn leads to increased RV afterload and further induces RV remodeling.[44] Right ventricular hypertrophy caused by this condition is a hallmark of human pulmonary hypertension. Therefore, we used RVHI as an indicator of PAH in the experimental model to assess right ventricular hypertrophy. In this experiment, we examined the effects of 18β-GA on mPAP, RVSP, and RVHI.[45] Our results suggested that 18β-GA-Lips (50 mg/kg) therapy inhibited the increase in mPAP, RVSP, and RVHI in a dose, administration, and delivery system-dependent manner.

Due to its reliability and noninvasiveness, echocardiography has gradually become an important auxiliary tool for diagnosing PAH.[46] The echocardiographic results are also positively correlated with those of right heart catheterization. In this study, the results showed that 18β-GA significantly improved abnormalities in PVmax, PAAT, and other echocardiographic parameters in PAH rats, with no significant difference.

Pulmonary vascular remodeling specifically involves the proliferation of pulmonary artery smooth muscle, abnormal proliferation of elastic and collagen fibers, thickening and hardening of the vascular wall, and lumen stenosis.[47,48] In this study, WT% and WA%, as shown by H&E staining, were used to evaluate pulmonary arteriolar vascular remodeling, and transmission electron microscopy was employed to analyze changes in the ultrastructure of the pulmonary artery.[49,50]. The pulmonary vascular medial wall thickness and vascular proliferation significantly increased in the SuHx-treated groups, which also served as indicators of PAH. 18β-GA can ameliorate the elevation of WT% and WA% in rat pulmonary arterioles caused by SuHx; in particular, atomized inhalation of 18β-GA-Lips (50 mg/kg) inhibited the increase in WT% and WA%. Microscopic observation of the ultrastructure of rat lung tissue revealed that rats in the SuHx group exhibited abnormal mitochondrial structure, vasoconstriction, capillary stenosis, and peripheral capillary edema. These changes were alleviated in the treatment groups. Based on the aforementioned microscopic observations, 18β-glycyrrhetinic acid solution and 18β-glycyrrhetinic acid liposomes partially inhibited and ameliorated the ultrastructural changes in lung tissue associated with vascular remodeling in the pulmonary arterial hypertension rat model. These findings were consistent with the results of pathological tissue morphology analysis, further supporting the potential therapeutic effects of 18β-glycyrrhetinic acid through its inhibition of pulmonary vascular remodeling. The results are consistent with previous studies on the effects of 18β-GA and isorhamnetin in MCT-induced PAH rat models, suggesting that our findings exhibit high reproducibility and hold promise for clinical application.[16,17,38]

Based on these results, 18β-GA-Lips, due to their appropriate size, can quickly reach the deep alveolar regions of the lung when inhaled, thereby increasing the accumulation of 18β-GA in the lung, providing prolonged retention, and releasing 18β-GA through cell fusion, improving its bioavailability and producing a concentration-dependent effect. This allows it to exert a better effect at a smaller dose. Although current research data have thoroughly confirmed the therapeutic efficacy of 18β-GA-Lips in pulmonary arterial hypertension and its notable advantages in lung-targeted delivery, future studies should prioritize a quantitative analysis of its impact on key PAH-associated signaling pathways and molecular factors, in order to systematically elucidate the potential molecular mechanisms underlying its therapeutic effects.

It is reasonable to conclude that the inhalation route has minimal effect on systemic symptoms, allowing the pharmacological activity of 18β-GA to be fully utilized, thereby improving the efficacy in PAH treatment. These results suggest that atomized inhalation of 18β-GA-Lips holds promising potential.

Conclusion

In this study, 18β-GA-Lips were successfully formulated, and their surface characteristics, pharmacokinetic profiles, tissue distribution, and lung-targeting capabilities were systematically evaluated. In the rat model of PAH induced by SuHx, both the 18β-GA solution and its liposomal formulation significantly improved hemodynamic parameters and alleviated right ventricular hypertrophy and cardiopulmonary injury. Notably, nebulized administration of 18β-GA-Lips at a dose of 50 mg/kg demonstrated enhanced therapeutic efficacy, which can be attributed to its low dosage requirement, convenient delivery method, and favorable pharmacokinetic properties. These findings provide a solid theoretical foundation and substantial experimental evidence for the application of 18β-GA-Lips in PAH treatment and introduce a novel and promising therapeutic strategy for clinical intervention.

Arrive (Animal Research: Reporting of In vivo Experiments) Statement

Male ICR mic (20 ± 2 g, 6 weeks old) and male Sprague-Dawley rats (220–250 g, 6 weeks old) were obtained from the Animal Experimental Center of Ningxia Medical University (SYXK Ningxia 2015-0001). The animal use protocol outlined below was reviewed and approved by the Laboratory Animal Ethical and Welfare Committee of the Laboratory Animal Center, Ningxia Medical University (IACUC-NYLAC-2020-015). All rats were housed in an animal room maintained at 20 ± 2°C with a humidity of 50%–60%. The light/dark cycle was set to 12 hours, and the animals had free access to food and water. The animal room is situated in the Key Laboratory of Ningxia Ethnic Medicine Modernization at Ningxia Medical University. All procedures related to feeding, modeling, administration, anesthesia, and other operations involving rats and mice in this experiment were conducted in the Key Laboratory of Ningxia Ethnic Medicine Modernization at Ningxia Medical University, which is an SPF-level environment. The study was conducted in accordance with the policies outlined in Basic & Clinical Pharmacology & Toxicology for experimental and clinical studies.

The animals used in all experiments were male, male mice and male SD rats. All animal experiments followed the ARRIVE guidelines.

Abbreviations

18β-GA-Lips, 18β-glycyrrhetinic acidliposomes; PAH, pulmonary arterial hypertension; GA, Glycyrrhetinic acid; UPLC/MS, Ultra Performance Liquid Chromatography Tandem Mass Spectrometry; SD rats, Sprague-Dawley rats; HSPC, hydrogenated soybean phospholipid; CHOL, cholesterol; DSPE-MPEG2000, distearoyl phosphatidylethanolamine polyethylene glycol 2000; HEPES, N-2 hydroxyethyl piperazine-n′- 2 ethanesulfonic acid; SDS, Sodium dodecyl sulfate; PDI, Polydispersity Index; NS, normal saline; Te, target efficiency; RTe, relative target efficiency; Re, relative uptake rate; Ce, peak concentration ratio; FOB, Functional Observation Battery; WBC, white blood cell; RBC, red blood cell count; HGB, hemoglobin; HCT, hematocrit; PLT, platelet count; MPV, mean platelet volume; PCT, plateletcrit; MCV, Mean corpuscular volume; MCH, mean corpuscular hemoglobin content; MCHC, mean corpuscular hemoglobin concentration; RDW, red blood cell distribution width; PDW, platelet distribution width; AST, Aspartate transaminase; ALT, alanine aminotransferase; T-BIL, total bilirubin; D-BIL, direct bilirubin; IBIL, indirect bilirubin; TP, total protein; ALP, Alkaline phosphatase; GLB, globulin; A/G, white/ball ratio; GGT, glutamyltransferase; BUN, urea; CRE, creatinine; GLU, Glucose; TG, Triglycerides; TCHO, Total cholesterol; HDL-C, High-density lipoprotein cholesterol; LDL-C, Low-density lipoprotein cholesterol; CK, Creatine kinase; CHE, cholinesterase; IP, Inorganic phosphorus; LDH, Lactate dehydrogenase; TBA, total Bile acid; UA, Uric acid; HR, heart rate; G/L, Specific gravity vitamin C; WBC, White blood cell; NIT, Nitrite; PRO, Protein; GLU, glucose; G/L, Vitamin C; KET, Ketone body; URO, Urobilinogen; BIL, Bilirubin; VS, systolic blood flow velocity; VD, diastolic blood flow velocity; SV, stroke volume; EF%, left ventricular Ejection fraction; FS%, left ventricular shortening fraction; CO, stroke output; LV Mass, left ventricular mass; G/L, Specific gravity vitamin C; NIT, nitrite; PVmax, The maximum pulmonary blood flow velocity; PAAT, pulmonary artery

acceleration time; PAD, pulmonary artery deceleration rate; RVESD, the end-systolic diameter of the right ventricle; RV, The right ventricle; LV + S, left ventricle + inter-ventricular septum; RVHI, The right ventricular hypertrophy index; H&E, hematoxylin and eosin; WT%, ratio of pulmonary arterial wall thickness; WA%, ratio of pulmonary arterial wall area; ANOVA, analysis of variance; EE, the enhanced permeability and retention; Enbedding Efficiency; EPR, enhanced permeability and retention; DL, drug loadings; IS, the internal standard; RVHI, the right ventricular hypertrophy index, VEGFR, the vascular endothelial growth factor receptor; TEM, Transmission Electron Microscopy.

Data Sharing Statement

Data is provided within the manuscript or supplementary information file.

Acknowledgments

This project was supported by the study on the mechanism, safety evaluation, and Formulation of 18β-glycyrrhetinic acid in the treatment of pulmonary arterial hypertension (Grant No:2019BFG02027); 2017 Ningxia Science and Technology Innovation Leader training project (Grant No. KJT2017005).

Author Contributions

Yanmin Pei: Writing – original draft, Formal analysis Validation. Meidong Si: Writing – original draft, Formal analysis, Investigation. Fang Zhao: Conceptualization, Methodology, Writing – review & editing. Ru Zhou: Conceptualization, Methodology, Funding acquisition, Writing – review & editing. Xuemei Ma: Data curation, Software, Validation. Siyun Liu: Investigation, Data curation, Software. Yanmin Pei, Meidong Si, Xuemei Ma, Siyun Liu, Fang Zhao, Ru Zhou: Revising the manuscript critically for important intellectual content.

All authors made a significant contribution to the work reported, whether that is in the conception, study design, execution, acquisition of data, analysis and interpretation, or in all these areas; took part in drafting, revising or critically reviewing the article; gave final approval of the version to be published; have agreed on the journal to which the article has been submitted; and agree to be accountable for all aspects of the work.

Disclosure

All authors have no known competing financial interests or personal relationships.

The work described has not been submitted elsewhere for publication, in whole or in part, and all the authors listed have approved the manuscript that is enclosed.

References

1. Benza RL, Gomberg-Maitland M, Elliott CG, et al. Predicting Survival in Patients With Pulmonary Arterial Hypertension: the REVEAL Risk Score Calculator 2.0 and Comparison With ESC/ERS-Based Risk Assessment Strategies. *Chest*. 2019;156(2):323–337. doi:10.1016/j.chest.2019.02.004
2. Bordenave J, Tu L, Savale L, Huertas A, Humbert M, Guignabert C. New insights in the pathogenesis of pulmonary arterial hypertension. *Rev Mal Respir*. 2019;36(4):433–437. doi:10.1016/j.rmr.2019.03.003
3. Global, regional, and national burden of pulmonary arterial hypertension, 1990-2021: a systematic analysis for the Global Burden of Disease Study 2021. *The Lancet. Respiratory medicine*. 2025;13(1):69–79. doi:10.1016/S2213-2600(24)00295-9.
4. Guignabert C, Aman J, Bonnet S, et al. Pathology and pathobiology of pulmonary hypertension: current insights and future directions. *Eur Respir J*. 2024;64(4):2401095. doi:10.1183/13993003.01095-2024
5. Mocumbi A, Humbert M, Saxena A, et al. Pulmonary hypertension. *Nat Rev Dis Primers*. 2024;10(1):1. doi:10.1038/s41572-023-00486-7
6. Lim Y, Low T, Chan S, et al. Pulmonary arterial hypertension in a multi-ethnic Asian population: characteristics, survival and mortality predictors from a 14-year follow-up study. *Respirology*. 2019;24(2):162–170. doi:10.1111/resp.13392
7. Quan R, Zhang G, Yu Z, et al. Characteristics, goal-oriented treatments and survival of pulmonary arterial hypertension in China: insights from a national multicentre prospective registry. *Respirology*. 2022;27(7):517–528. doi:10.1111/resp.14247
8. El-Kersh K, Jalil BA. Pulmonary hypertension inhaled therapies: an updated review. *Am J Med Sci*. 2023;366(1):3–15. doi:10.1016/j.amjms.2023.03.002
9. Guglielmi G, Dimopoulos K, Wort SJ. New therapies in pulmonary arterial hypertension: recent insights. *Int J Cardiol Congenit Heart Dis*. 2025;19:100571.
10. Vaidya B, Gupta V. Novel therapeutic approaches for pulmonary arterial hypertension: unique molecular targets to site-specific drug delivery. *J Control Release*. 2015;211:118–133. doi:10.1016/j.jconrel.2015.05.287
11. Garcia-Mouton C, Hidalgo A, Cruz A, Perez-Gil J. The Lord of the Lungs: the essential role of pulmonary surfactant upon inhalation of nanoparticles. *Eur J Pharm Biopharm*. 2019;144:230–243. doi:10.1016/j.ejpb.2019.09.020

12. Zhang Q, Lee SB, Chen X, et al. Optimized Bexarotene Aerosol Formulation Inhibits Major Subtypes of Lung Cancer in Mice. *Nano Lett*. 2019;19(4):2231–2242. doi:10.1021/acs.nanolett.8b04309
13. Franek F, Fransson R, Thorn H, Backman P, Andersson PU, Tehler U. Ranking *in Vitro* Dissolution of Inhaled Micronized Drug Powders including a Candidate Drug with Two Different Particle Sizes. *Mol Pharm*. 2018;15(11):5319–5326. doi:10.1021/acs.molpharmaceut.8b00796
14. Singh C, Koduri LVSK, Dhawale V, et al. Potential of aerosolized rifampicin lipospheres for modulation of pulmonary pharmacokinetics and bio-distribution. *Int J Pharm*. 2015;495(2):627–632. doi:10.1016/j.ijpharm.2015.09.036
15. Sun J, Liu H, Lv C, Qin J, Modification WY. Antitumor Activity, and Targeted PPARgamma Study of 18beta-Glycyrrhetinic Acid, an Important Active Ingredient of Licorice. *J Agric Food Chem*. 2019;67(34):9643–9651. doi:10.1021/acs.jafc.9b03442
16. Zhang M, Chang Z, Zhang P, et al. Protective effects of 18beta-glycyrrhetinic acid on pulmonary arterial hypertension via regulation of Rho A/Rho kinase pathway. *Chem Biol Interact*. 2019;311:108749. doi:10.1016/j.cbi.2019.108749
17. Zhang M, Chang Z, Zhao F, et al. Protective Effects of 18beta-Glycyrrhetinic Acid on Monocrotaline-Induced Pulmonary Arterial Hypertension in Rats. *Front Pharmacol*. 2019;10:13. doi:10.3389/fphar.2019.00013
18. Liu T, Zhu W, Han C, et al. Preparation of Glycyrrhetinic Acid Liposomes Using Lyophilization Monophase Solution Method: preformulation, Optimization, and *In Vitro* Evaluation. *Nanoscale Res Lett*. 2018;13(1):324. doi:10.1186/s11671-018-2737-5
19. Chen J, Chen Y, Cheng Y, et al. Modifying glycyrrhetinic acid liposomes with liver-targeting ligand of galactosylated derivative: preparation and evaluations. *Oncotarget*. 2017;8(60):102046–102066. doi:10.18632/oncotarget.22143
20. Li S, Qiu YQ, Zhang SH, Gao YH. A novel transdermal fomulation of 18beta-glycyrrhetic acid with lysine for improving bioavailability and efficacy. *Skin Pharmacol Physiol*. 2012;25(5):257–268. doi:10.1159/000339652
21. Liang S, Li M, Yu X, et al. Synthesis and structure-activity relationship studies of water-soluble beta-cyclodextrin-glycyrrhetinic acid conjugates as potential anti-influenza virus agents. *Eur J Med Chem*. 2019;166:328–338. doi:10.1016/j.ejmech.2019.01.074
22. Quan W, Kong S, Ouyang Q, et al. Use of 18beta-glycyrrhetinic acid nanocrystals to enhance anti-inflammatory activity by improving topical delivery. *Colloids Surf B Biointerfaces*. 2021;205:111791. doi:10.1016/j.colsurfb.2021.111791
23. Tveden-Nyborg P, Bergmann TK, Jessen N, Simonsen U, Lykkesfeldt J. BCPT 2023 policy for experimental and clinical studies. *Basic Clin Pharmacol Toxicol*. 2023;133(4):391–396. doi:10.1111/bcpt.13944
24. Chen J, Lin Y, Wu M, et al. Drug-Free Liposomes Containing Mannosylated Ligand for Liver-Targeting: synthetic Optimization, Liposomal Preparation, and Bioactivity Evaluation. *J Biomed Nanotechnol*. 2021;17(12):2455–2465. doi:10.1166/jbn.2021.3204
25. Zhang Y, Xiong Y, Wu X, et al. Injectable Hydrogel With Glycyrrhizic Acid and Asiaticoside-Loaded Liposomes for Wound Healing. *J Cosmet Dermatol*. 2024;23(12):3927–3935. doi:10.1111/jocd.16606
26. Chen J, Chen Y, Cheng Y, Gao Y. Glycyrrhetinic Acid Liposomes Containing Mannose-Diester Lauric Diacid-Cholesterol Conjugate Synthesized by Lipase-Catalytic Acylation for Liver-Specific Delivery. *Molecules*. 2017;22(10):1598. doi:10.3390/molecules22101598
27. Chen J, Lin Y, Wu M, et al. Glycyrrhetinic acid proliposomes mediated by mannosylated ligand: preparation, physicochemical characterization, environmental stability and bioactivity evaluation. *Colloids Surf B Biointerfaces*. 2022;218:112781. doi:10.1016/j.colsurfb.2022.112781
28. Hamill RJ. Amphotericin B formulations: a comparative review of efficacy and toxicity. *Drugs*. 2013;73(9):919–934. doi:10.1007/s40265-013-0069-4
29. Liu M, Li J, Zhao D, et al. Branched PEG-modification: a new strategy for nanocarriers to evade of the accelerated blood clearance phenomenon and enhance anti-tumor efficacy. *Biomaterials*. 2022;283:121415. doi:10.1016/j.biomaterials.2022.121415
30. Bae S, Lee S. Synthesis of Gold Nanoflowers Encapsulated with Poly(N-isopropylacrylamide-co-acrylic acid) Hydrogels. *J Nanosci Nanotechnol*. 2015;15(10):7962–7965. doi:10.1166/jnn.2015.11232
31. Gandhi M, Pandya T, Gandhi R, et al. Inhalable liposomal dry powder of gemcitabine-HCl: formulation, *in vitro* characterization and *in vivo* studies. *Int J Pharm*. 2015;496(2):886–895. doi:10.1016/j.ijpharm.2015.10.020
32. Xu S, Su H, Zhu X, et al. Long-circulating doxorubicin and schizandrin A liposome with drug-resistant liver cancer activity: preparation, characterization, and pharmacokinetic. *J Liposome Res*. 2022;32(2):107–118. doi:10.1080/08982104.2021.1884093
33. Marante T, Viegas C, Duarte I, Macedo AS, Fonte P. An Overview on Spray-Drying of Protein-Loaded Polymeric Nanoparticles for Dry Powder Inhalation. *Pharmaceutics*. 2020;12(11):1032. doi:10.3390/pharmaceutics12111032
34. Thorley AJ, Ruenraroengsak P, Potter TE, Tetley TD. Critical determinants of uptake and translocation of nanoparticles by the human pulmonary alveolar epithelium. *ACS Nano*. 2014;8(11):11778–11789. doi:10.1021/nn505399e
35. Agertoft L, Laulund LW, Harrison LI, Pedersen S. Influence of particle size on lung deposition and pharmacokinetics of beclomethasone dipropionate in children. *Pediatr Pulmonol*. 2003;35(3):192–199. doi:10.1002/ppul.10238
36. Liu J, Deng Y, Fu D, et al. Sericin microparticles enveloped with metal-organic networks as a pulmonary targeting delivery system for intra-tracheally treating metastatic lung cancer. *Bioact Mater*. 2021;6(1):273–284. doi:10.1016/j.bioactmat.2020.08.006
37. Alexander BD, Winkler TP, Shi S, Dodds Ashley ES, Hickey AJ. *In vitro* characterization of nebulizer delivery of liposomal amphotericin B aerosols. *Pharm Dev Technol*. 2011;16(6):577–582. doi:10.3109/10837450.2011.591803
38. Chang Z, Wang J, Jing Z, et al. Protective effects of isorhamnetin on pulmonary arterial hypertension: *in vivo* and *in vitro* studies. *Phytother Res*. 2020;34(10):2730–2744. doi:10.1002/ptr.6714
39. Yun X, Philip NM, Jiang H, et al. Upregulation of Aquaporin 1 Mediates Increased Migration and Proliferation in Pulmonary Vascular Cells From the Rat SU5416/Hypoxia Model of Pulmonary Hypertension. *Front Physiol*. 2021;12:763444. doi:10.3389/fphys.2021.763444
40. Liu P, Huang W, Ding Y, et al. Fasudil Dichloroacetate Alleviates SU5416/Hypoxia-Induced Pulmonary Arterial Hypertension by Ameliorating Dysfunction of Pulmonary Arterial Smooth Muscle Cells. *Drug Des Devel Ther*. 2021;15:1653–1666. doi:10.2147/DDDT.S297500
41. Sanada TJ, Hosomi K, Park J, et al. Partially hydrolyzed guar gum suppresses the progression of pulmonary arterial hypertension in a SU5416/hypoxia rat model. *Pulm Circ*. 2023;13(3):e12266. doi:10.1002/pul2.12266
42. Imano H, Kato R, Nomura A, et al. Rivaroxaban Attenuates Right Ventricular Remodeling in Rats with Pulmonary Arterial Hypertension. *Biol Pharm Bull*. 2021;44(5):669–677. doi:10.1248/bpb.b20-01011
43. Mamazhakypov A, Weiss A, Zukunft S, et al. Effects of macitentan and tadalafil monotherapy or their combination on the right ventricle and plasma metabolites in pulmonary hypertensive rats. *Pulm Circ*. 2020;10(4):765600429. doi:10.1177/2045894020947283
44. Sanchez-Gloria JL, Martinez-Olivares CE, Del Valle-Mondragon L, et al. Allicin, an Emerging Treatment for Pulmonary Arterial Hypertension: an Experimental Study. *Int J Mol Sci*. 2023;24(16):12959. doi:10.3390/ijms241612959

45. He M, Zhang Y, Xie F, Dou X, Han M, Zhang H. Role of PI3K/Akt/NF-kappaB and GSK-3beta pathways in the rat model of cardiopulmonary bypass-related lung injury. *Biomed Pharmacother*. 2018;106:747–754. doi:10.1016/j.biopha.2018.06.125
46. G LYL, Tepox galicia AY, Atonal Flores F, et al. Echocardiographic follow-up to right ventricular modifications in secondary pulmonary hypertension to diabetes in rats. *Clin Exp Hypertens*. 2021;43(3):242–253. doi:10.1080/10641963.2020.1860077
47. Zhang S, Liu X, Ge LL, et al. Mesenchymal stromal cell-derived exosomes improve pulmonary hypertension through inhibition of pulmonary vascular remodeling. *Respir Res*. 2020;21(1):71. doi:10.1186/s12931-020-1331-4
48. Pan T, Zhang L, Miao K, Wang Y. A crucial role of endoplasmic reticulum stress in cellular responses during pulmonary arterial hypertension. *Am J Transl Res*. 2020;12(5):1481–1490.
49. Prisco SZ, Hartweck LM, Rose L, et al. Inflammatory Glycoprotein 130 Signaling Links Changes in Microtubules and Junctophilin-2 to Altered Mitochondrial Metabolism and Right Ventricular Contractility. *Circ Heart Fail*. 2022;15(1):e8574. doi:10.1161/CIRCHEARTFAILURE.122.009570
50. Cerecedo D, Martinez-Vieyra I, Lopez-Villegas EO, Hernandez-Cruz A, Loza-Huerta ADC. Heterogeneity of neutrophils in arterial hypertension. *Exp Cell Res*. 2021;402(2):112577. doi:10.1016/j.yexcr.2021.112577